U.S. Department
of Transportation
Federal Railroad
Administration

Office of Research,
Development and Technology
Washington, DC 20590

LiDAR Grade Crossing Data Collection and Storage Services for High Profile Grade Crossings

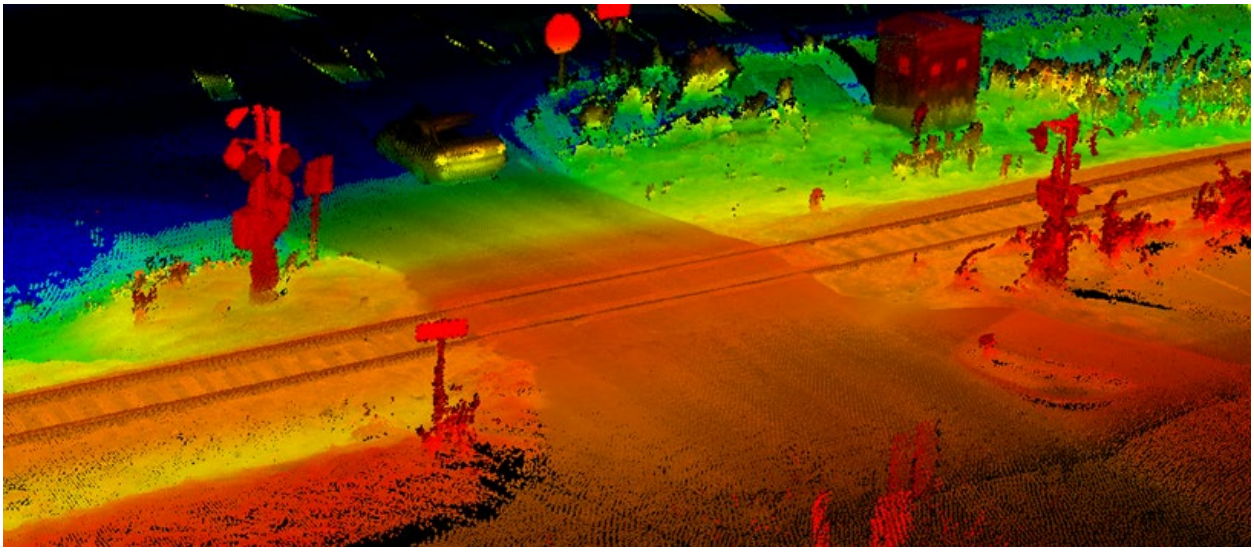

DOT/FRA/ORD-24/40

Final Report | September 2024

REPORT DOCUMENTATION PAGE

Form Approved
OMB No. 0704-0188

1. REPORT DATE *(DD-MM-YYYY)*	**2. REPORT TYPE**	**3. DATES COVERED** *(From - To)*
	Technical Report	8/18/2022 – 12/18/2023

4. TITLE AND SUBTITLE

LiDAR Grade Crossing Data Collection and Storage Services for High Profile Grade Crossings

5a. CONTRACT NUMBER

5b. GRANT NUMBER

5c. PROGRAM ELEMENT NUMBER

6. AUTHOR(S)

Sean Woods #0009-0007-2513-0070

Jeff Meunier #0000-0000-0000-0000

5d. PROJECT NUMBER

5e. TASK NUMBER

5f. WORK UNIT NUMBER

7. PERFORMING ORGANIZATION NAME(S) AND ADDRESS(ES)
ENSCO, Inc.
Applied Technology and Engineering Division
5400 Port Royal Road
Springfield, VA 22151

8. PERFORMING ORGANIZATION REPORT NUMBER

If Any

9. SPONSORING/MONITORING AGENCY NAME(S) AND ADDRESS(ES)
U.S. Department of Transportation
Federal Railroad Administration
Office of Railroad Policy and Development
Office of Research, Development, and Technology
Washington, DC 20590

10. SPONSOR/MONITOR'S ACRONYM(S)

11. SPONSOR/MONITOR'S REPORT NUMBER(S)
DOT/FRA/ORD-24/40

12. DISTRIBUTION/AVAILABILITY STATEMENT
This document is available to the public through the FRA website.

13. SUPPLEMENTARY NOTES
COR: Francesco Bedini

14. ABSTRACT

This report summarizes work performed to improve identification of high-profile grade crossings throughout the nation's railway network.

In May 2019 two rail survey vehicles operated under the FRA Office of Safety's Automated Track Inspection Program were equipped with LiDAR 3D scanner arrays that automatically measure the profile of grade crossings. Following a year and a half of data collection, FRA identified several types of crossings that did not reliably record accurate measurements. FRA contracted with a research team from ENSCO, Inc. to update the data processing algorithms used to analyze this data. The work performed under this task focused on refinements to the data processing algorithms used to extract measurements from the point clouds, particularly under challenging circumstances such as grade crossings with acute roadway angles, intersections with complex roadway layouts, and crossings surrounded by heavy vegetation.

15. SUBJECT TERMS
LIDAR, GRADE CROSSING, MOTORIST SAFETY, ATIP

16. SECURITY CLASSIFICATION OF:			**17. LIMITATION OF ABSTRACT**	**18. NUMBER OF PAGES**	**19a. NAME OF RESPONSIBLE PERSON**
a. REPORT	**b. ABSTRACT**	**c. THIS PAGE**		75	**19b. TELEPHONE NUMBER** *(Include area code)*

Standard Form 298 (Rev. 8/98)
Prescribed by ANSI Std. Z39.18

METRIC/ENGLISH CONVERSION FACTORS

ENGLISH TO METRIC	METRIC TO ENGLISH
LENGTH (APPROXIMATE)	**LENGTH (APPROXIMATE)**
1 inch (in) = 2.5 centimeters (cm)	1 millimeter (mm) = 0.04 inch (in)
1 foot (ft) = 30 centimeters (cm)	1 centimeter (cm) = 0.4 inch (in)
1 yard (yd) = 0.9 meter (m)	1 meter (m) = 3.3 feet (ft)
1 mile (mi) = 1.6 kilometers (km)	1 meter (m) = 1.1 yards (yd)
	1 kilometer (km) = 0.6 mile (mi)
AREA (APPROXIMATE)	**AREA (APPROXIMATE)**
1 square inch (sq in, in^2) = 6.5 square centimeters (cm^2)	1 square centimeter (cm^2) = 0.16 square inch (sq in, in^2)
1 square foot (sq ft, ft^2) = 0.09 square meter (m^2)	1 square meter (m^2) = 1.2 square yards (sq yd, yd^2)
1 square yard (sq yd, yd^2) = 0.8 square meter (m^2)	1 square kilometer (km^2) = 0.4 square mile (sq mi, mi^2)
1 square mile (sq mi, mi^2) = 2.6 square kilometers (km^2)	10,000 square meters (m^2) = 1 hectare (ha) = 2.5 acres
1 acre = 0.4 hectare (he) = 4,000 square meters (m^2)	
MASS - WEIGHT (APPROXIMATE)	**MASS - WEIGHT (APPROXIMATE)**
1 ounce (oz) = 28 grams (gm)	1 gram (gm) = 0.036 ounce (oz)
1 pound (lb) = 0.45 kilogram (kg)	1 kilogram (kg) = 2.2 pounds (lb)
1 short ton = 2,000 pounds (lb) = 0.9 tonne (t)	1 tonne (t) = 1,000 kilograms (kg) = 1.1 short tons
VOLUME (APPROXIMATE)	**VOLUME (APPROXIMATE)**
1 teaspoon (tsp) = 5 milliliters (ml)	1 milliliter (ml) = 0.03 fluid ounce (fl oz)
1 tablespoon (tbsp) = 15 milliliters (ml)	1 liter (l) = 2.1 pints (pt)
1 fluid ounce (fl oz) = 30 milliliters (ml)	1 liter (l) = 1.06 quarts (qt)
1 cup (c) = 0.24 liter (l)	1 liter (l) = 0.26 gallon (gal)
1 pint (pt) = 0.47 liter (l)	
1 quart (qt) = 0.96 liter (l)	
1 gallon (gal) = 3.8 liters (l)	
1 cubic foot (cu ft, ft^3) = 0.03 cubic meter (m^3)	1 cubic meter (m^3) = 36 cubic feet (cu ft, ft^3)
1 cubic yard (cu yd, yd^3) = 0.76 cubic meter (m^3)	1 cubic meter (m^3) = 1.3 cubic yards (cu yd, yd^3)
TEMPERATURE (EXACT)	**TEMPERATURE (EXACT)**
[(x-32)(5/9)] °F = y °C	[(9/5) y + 32] °C = x °F

QUICK INCH - CENTIMETER LENGTH CONVERSION

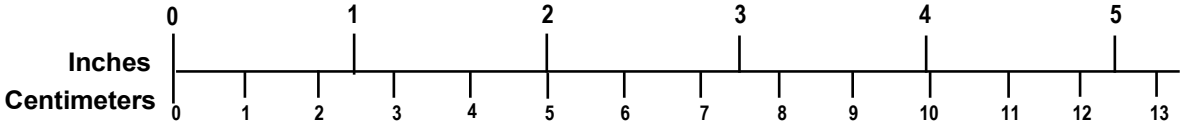

QUICK FAHRENHEIT - CELSIUS TEMPERATURE CONVERSIO

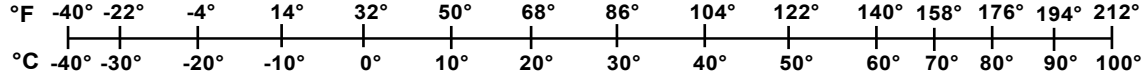

For more exact and or other conversion factors, see NIST Miscellaneous Publication 286, Units of Weights and Measures. Price $2.50 SD Catalog No. C13 10286

Updated 6/17/98

Acknowledgements

The authors acknowledge the support provided by the Automated Track Inspection Program operated by the Federal Railroad Administration's Office of Safety. Their generous offer to use their existing survey vehicles as a platform to collect LiDAR data made this research to advance detection of potentially hazardous grade crossings possible.

Contents

Illustrations

Tables

Executive Summary

Collisions between motor vehicles and trains are a leading cause of injuries in the railroad industry. From 2017 through 2023 there were a total of 13,449 grade crossing incidents involving all types of vehicles, resulting in 1,385 fatalities and 4,486 injuries. A major cause of grade crossing incidents are vehicle hangups due to high-profile (i.e., "humped") grade crossings. To address this issue, the Federal Railroad Administration (FRA) has worked to improve their ability to identify high-profile grade crossings and increase awareness of sites that pose a risk to motorists.

In May 2019 two rail survey vehicles operated under the FRA Office of Safety's Automated Track Inspection Program (ATIP) were equipped with LiDAR 3D scanner arrays that automatically measure the profile of grade crossings. Following a year and a half of data collection, FRA identified several types of crossings that did not reliably record accurate measurements.

FRA contracted with a research team from ENSCO, Inc. to update the data processing algorithms used to analyze this data. The team reprocessed the data using the updated algorithms to improve accuracy at crossings with sharp roadway intersection angles, multiple tracks in the crossings, or heavy vegetation near the crossing. A manual review process demonstrated the system to have a median error of 32 mm (1.26 inches), sufficient for the intended use of identifying humped crossings.

The research team also analyzed coverage of the LiDAR equipped vehicles nationwide and worked to evaluate alternate methods of collecting grade crossing information at locations unlikely to be surveyed through the ATIP program. The team evaluated the Crossing-i system developed by Michigan Technological Research Institute, which uses drone-based imagery to create a 3-D point cloud like that produced using a LiDAR scanner. While the Crossing-I system is more time-consuming and expensive to operate than the LiDAR system onboard ATIP vehicles, it can be used to provide targeted measurements at crossings where no other methods are likely to be used.

The team found that no single method of inspection is likely to provide complete coverage of the vast network of rail crossings in the United States. Considering the risk to motorists as well as the efficient operation of the nation's rail network, continued research is needed to improve identification of humped crossings.

1 Introduction

This report summarizes work performed to improve identification of high-profile grade crossings throughout the nation's railway network.

In May 2019 two rail survey vehicles operated under the Federal Railroad Administration (FRA) Office of Safety's Automated Track Inspection Program (ATIP) were equipped with LiDAR 3D scanner arrays that automatically measure the profile of grade crossings. Following a year and a half of data collection, FRA identified several types of crossings that did not reliably record accurate measurements.

FRA contracted with a research team from ENSCO, Inc. to update the data processing algorithms used to analyze this data. The work performed under this task focused on refinements to the data processing algorithms used to extract measurements from the point clouds, particularly under challenging circumstances such as grade crossings with acute roadway angles, intersections with complex roadway layouts, and crossings surrounded by heavy vegetation.

1.1 Background

Vehicle hang-ups at high profile grade crossings (HPGCs), or humped crossings, present a particular danger to the railroad industry. A hang-up can occur when a low clearance vehicle bottoms out on a humped crossing and becomes stuck across the right-of-way, or when a vehicle bumper drags the ground on a sagged crossing. Once a hang-up occurs, little can be done to prevent a collision. FRA works with the Federal Highway Administration (FHWA) to minimize the occurrence of hang-ups at HPGCs and to identify other grade crossing hazards that present a risk to public safety.

Under a prior task order, FRA developed a system that would effectively capture the profile of grade crossings using LiDAR sensors. This system was deployed on DOTX 220 and DOTX 304 survey vehicles operated under ATIP. As the vehicles perform normal survey operations, the onboard LiDAR system collects point cloud data and automatically identifies HPGCs as the vehicle(s) traverse at-grade crossings. Post-processing of the data extracts the vertical deviation of the roadway relative to the tracks, known as the planer deviation.

FRA validates the LiDAR measurements and supports ongoing collection of the data. Modifications to the data processing algorithms used to calculate grade crossing profiles would improve accuracy over the wide range of existing crossing configurations. Additionally, efforts are needed to automate the transfer, processing, and storage of LiDAR data collected by FRA.

1.2 Objectives

The main objective of this task was to build on previous research using LiDAR measurement technology to improve identification of HPGCs. An additional objective was to improve data storage methods to facilitate data-sharing with industry engineers and academic researchers. Specifically, this objective included:

1. Improve the accuracy of planer deviations measurements collected at grade crossings.
2. Conduct stakeholder outreach to better understand the needs of end-users in industry and academia.

3. Migrate post-processing of the collected LiDAR point clouds onto the collection vehicle(s).

1.3 Overall Approach

To achieve the objectives described above, researchers performed a manual review of previously processed grade crossing point clouds that were reported to have high planer deviations. Identification of grade crossings that contain characteristics which are a challenge for the existing algorithms, along with the true planer deviation values obtained manually, provide a sample dataset that was used to refine and test the processing algorithms.

1.4 Scope

The research team focused their efforts on analysis of previously collected grade crossing point clouds and improvements to the data processing algorithms used to determine the planer deviation. Additionally, the team worked to transform the data workflow from batch processing to low-latency onboard processing and automated data transfer to a cloud hosted storage solution. Lastly, an evaluation of non-rail-based surveying methods was conducted to identify possible methods of collecting planer deviation data at grade crossings unlikely to be surveyed by ATIP vehicles.

1.5 Organization of the Report

Section 2 contains a discussion of industry standards for highway grade crossings, maintenance considerations, and the motivation to improve detection of humped crossings. Section 3 summarizes the scope of work included under this effort and the researchers' approach. A detailed discussion of algorithm improvements, validation of the measurements, and evaluation of other inspection methods is provided in Section 4. Summary of the work and relevant findings are included in Section 5.

2 Industry Standards and Motivation

The vertical profile of the roadway through a grade crossing should be as level as possible. This reduces the risk of a hangup for passing vehicles. Long wheelbase, low-clearance trailers pose the greatest risk of becoming stuck while navigating a grade crossing. Although construction and maintenance standards vary between municipalities and are influenced by the expected type and volume of vehicular traffic, there are recommended standards in place for highway grade crossings.

2.1 Highway Grade Crossing Standards and Evolving Track Conditions

The American Association of State Highway and Transportation Officials (AASHTO) has established a guideline for the vertical profile of the roadway at grade crossings. This guideline has also been adopted by the American Railway Engineering and Maintenance-of-Way Association (AREMA). The AASHTO guideline shown in Figure 1 can be traversed by a wide-range of roadway vehicles including those with long-wheelbase and low ground clearance. The guideline recommends that the roadway surface be in-plane with the top-of-rails for 2 feet on both sides of the track. Beyond 2 feet from the track, the roadway may not exceed 3 inches of vertical deviation 30 feet from either rail.

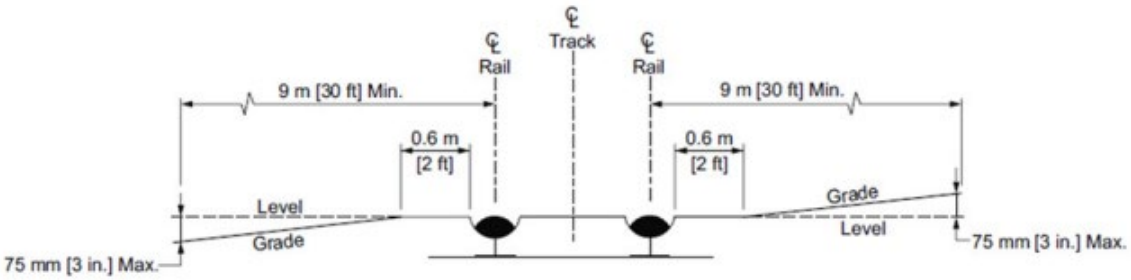

Figure 1: Maximum planer deviation of the railway as recommended by AASHTO

The guideline above is the recommended best practice for construction of new grade crossings; however, common constraints (e.g., drainage requirements, existing topography, and resource limitations) may prevent grade crossings over time from adhering to the recommended vertical profile. Crossings with a vertical profile exceeding the recommended 3 inches are flagged with high-profile signage to warn motorists of the elevated risk of a vehicle hangup.

Repeated track maintenance activities may raise the track over time (e.g., ballast added under the ties). The gradual change in elevation may result in a previously compliant crossing becoming higher in the middle, or "humped." Similarly, successive roadway maintenance may result in a layer of asphalt being added to the road surface. Over time the roadway approaches may become taller than the grade crossing, resulting in a "sag" crossing. This condition can cause vehicle bumpers or trailers to drag and become stuck.

2.2 Risk of Vehicle Collisions

Due to the long stopping distance required for typical rail traffic, it is critical that any vehicle entering a grade crossing be able to clear the crossing quickly. If a vehicle becomes stuck in the crossing, approaching rail traffic may not be able to stop before a collision occurs. Figure 2

shows a common humped crossing being negotiated by a passenger sedan. Humped crossings typically do not pose a significant risk to passenger vehicles except in the most extreme cases because their short wheelbase and typical ground clearance reduces the chance of the vehicle undercarriage becoming stuck on the tracks or adjacent roadway surfaces.

Figure 2: A humped high-profile grade crossing being negotiated by a passenger vehicle

However, humped crossings can pose a significant risk to the passage of long, low-clearance vehicles such as automobile transport trailers, heavy equipment transports, and other low-clearance trailers. Figure 3 shows an automobile transport trailer that has become stuck on a humped crossing. As these vehicles pass across the grade crossing, their long wheelbases cause the supporting axles to contact the roadway at points on either side of the tracks. When both contacts points are lower than the tracks, in the case of a humped crossing, more undercarriage clearance is required to pass over the crossing. This can result in long-wheelbase, low-clearance vehicles becoming struck on the tracks.

Figure 3: A automobile transport trailer stuck on a humped high-profile grade crossing

Collisions involving trains and road vehicles are extremely dangerous for motorists because of the weight and speed/energy of typical rail vehicles. Ideally, motorist exit their vehicle immediately after becoming stranded in a crossing, but this does not always happen, or the vehicle becomes stuck immediately before a collision. The later scenario is common when a motorist attempts to cross in front of an oncoming train, often the result of misjudging the distance or speed of the train. Typically, the motor vehicle involved in the collision is destroyed (Figure 4).

Figure 4: The remainder of a semi-truck involved in a train collision

Collisions with motor vehicles also present a significant risk to trains. Following a collision, a train may derail if the vehicle debris is trapped under the train, resulting in injury or loss of life to the train crew and/or passengers, significant damage to the track infrastructure, and other complications such as the release of hazardous materials carried as cargo. A notable collision occurred on June 27, 2022, when an Amtrak passenger train struck a dump-truck that was stranded on a humped crossing in rural Missouri (Figure 5). The collision resulted in the derailment of the Amtrak train and caused four fatalities and 150 injuries, 40 of which required hospitalization. The crossing involved in this incident was a passive crossing, protected only by crossbuck signage. In addition to being a humped HPGC, the intersection angle between the roadway and track, as well as the presence of overgrown vegetation, severely limited motorists' line-of-sight toward the approaching train.

Figure 5: An Amtrak train that derailed after striking a dump truck stuck in a humped crossing

In recent years the total number of grade crossing incidents has remained steady, with no appreciable decrease year over year (Table 1 and Figure 6). From 2017 through 2022 (the latest full year with available data) the average number of grade crossing incidents was 2,001, with the numbers for individual years showing very little deviation from the average. In total, during the 2017-2023 period there were 13,449 incidents involving all types of vehicles. These incidents resulted in 1,385 fatalities and 4,486 injuries. Considering the risk to motorists at HPGC incidents, FRA continues to evaluate methods to proactively identify potentially hazardous grade crossing and encourage mitigation measures to reduce the incidence of highway-rail traffic incidents.

Table 1: Number of grade crossing incidents per year (Source: FRA Highway/Rail Grade Crossing Incident Dashboard)

Calendar Year	Total Incidents
2017	1,971
2018	2,077
2019	2,082
2020	1,800
2021	2,029
2022	2,046
2023*	1,444

*Note: 2023 data includes incidents through December 1, 2023

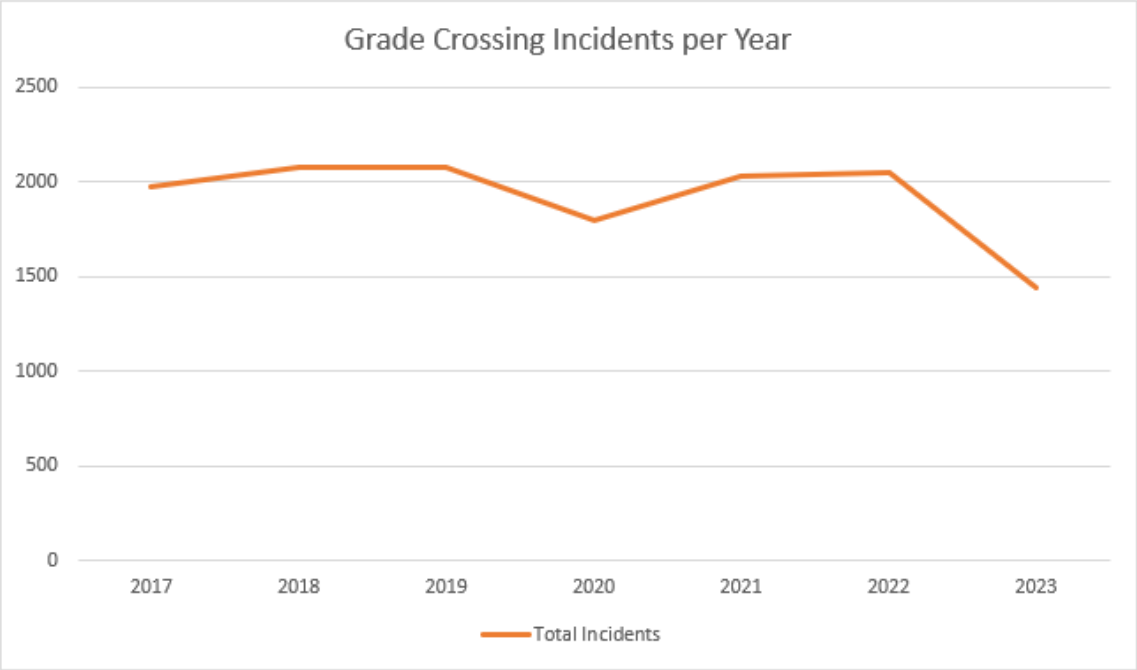

Figure 6: Grade crossing incidents per year

2.3 Motivation

The vertical profile of a grade crossing is an important consideration after track or roadway maintenance, which may inadvertently create a HPGC. If a crossing is found to be classified as high-profile, appropriate signage can be installed to warn motorists of the risk. Using a survey crew to resurvey crossings after maintenance and verify the vertical profile is within guidelines may be cost prohibitive for many municipalities, particularly in rural areas. Therefore, a method is needed to periodically measure the vertical profile of grade crossings in a cost-effective manner.

This goal motivated FRA to create the initial LiDAR grade crossing systems that were installed on DOTX220 and DOTX304 railcars in 2019. Analysis of data collected from May 2019 through September 2020 indicated that there were aspects of the system that could be modified to improve accuracy (see Figure 7).

In one notable finding, the distribution of planer deviation measurements produced by the systems did not have a normal distribution as expected. The distribution showed a significant spike in the occurrence of crossings with a planer deviation of approximately 0.5 meter.

A manual review of surveyed grade crossing sites was undertaken to quantify the accuracy of the LiDAR system results and better understand grade crossing characteristics that were likely to result in less accurate results.

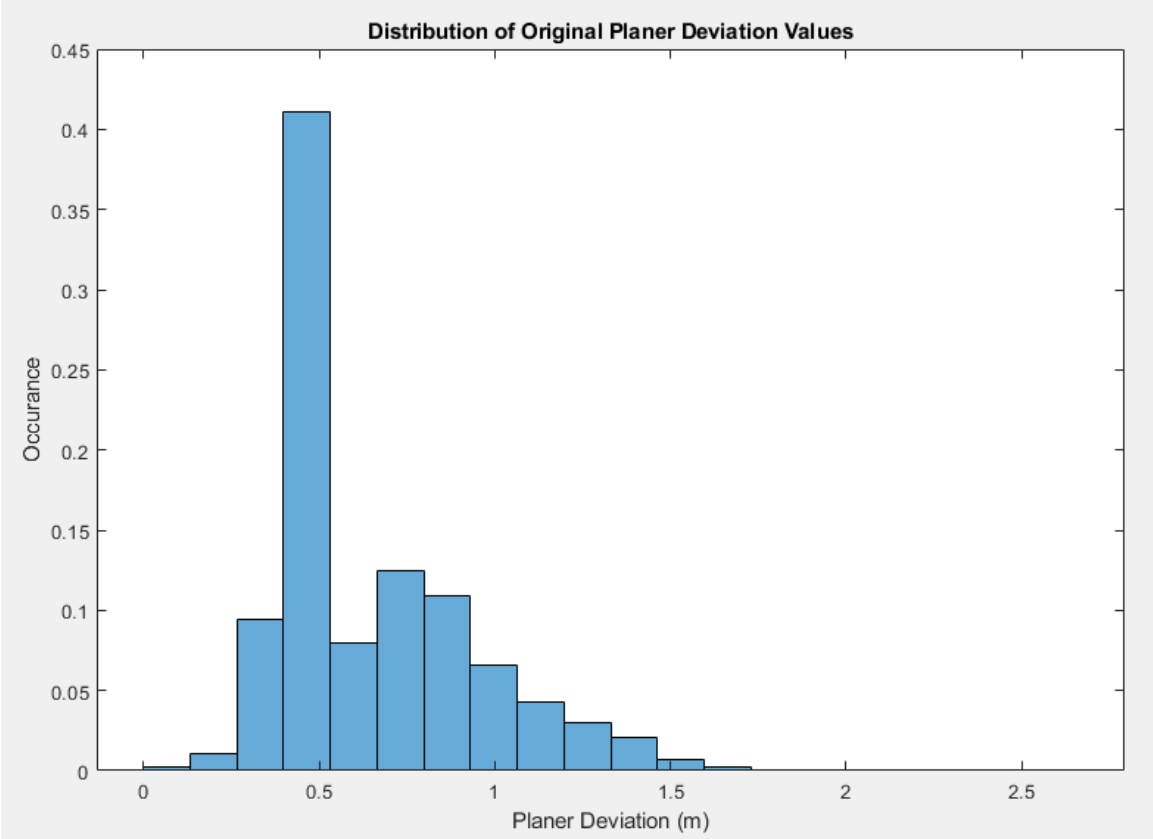

Figure 7: Distribution of grade crossing planer deviation values collected in 2019 and 2020

3 Methodology

This research included four primary areas of focus: 1) stakeholder outreach to potential data users to better understand the needs of industry professionals and academic researchers; 2) improvements to the previously developed data processing algorithms; 3) streamlining the data processing and transfer mechanism; and 4) evaluating other methods of collecting grade crossing profile measurements at crossings unlikely to be surveyed by ATIP vehicles.

3.1 Stakeholder Outreach

Prior to making updates to the data processing algorithms and developing a means of transferring and storing the grade crossing point clouds, it was critical to understand how the data would be used. Since FRA intends to make the point cloud data available to industry and academia, the data format, point cloud extents along the track and roadway, and data resolution must be sufficient for the intended applications.

FRA identified industry stakeholders who have either expressed interest in using the data or are actively performing research related to grade crossing safety. The selected stakeholders included railroad professionals, industry committees, academic researchers, FRA employees, and members of various states' Departments of Transportation and Highway. By involving a broad spectrum of potential data users, the research team worked to develop an understanding of the potential uses of the data and the impact of the data storage format .

A survey was developed that described the intended approach and requested feedback in critical areas. Specifically, feedback was requested regarding the following items:

- Data file format – The file extension type and associate software packages capable of accessing the data
- LiDAR point cloud extents – The length of the scan data along the track and along the roadway
- Metadata – Location, ownership info, and other metadata associated with each scanned crossing
- Planer deviation measurement – Format, units, and level of detail associated with the measurements derived from the point cloud scans

The team distributed the survey to the identified stakeholders. The full survey is included in Appendix A. The full list of stakeholders who received the survey is included in Appendix B.

A summary of the feedback received for each of the primary topics is provided below.

3.1.1 Data File Format

The team proposed to use a .LAZ file format for point cloud data. .LAZ is an open-source, compressed file format that can be viewed by several free software packages. It also uses common data processing languages such as Python or MATLAB. No stakeholders requested a proprietary format, although there was a request to use the .LAS file format because it is the ESRI standard (.LAS is the uncompressed equivalent of .LAZ and results in approximately 10 times larger data files). Both file types can be read by common open-source data viewers and conversion between the two formats is straight-forward. To reduce the volume of data being

transferred through the cellular connection, as well as reduce long-term storage and retrieval requirements, the team selected the transmission and storage of a compressed .LAZ point cloud.

3.1.2 Point Cloud Extents

A stakeholder indicated that detection of overhead utilities and other overhead obstructions in or near the crossing would be helpful data. Unfortunately, the LiDAR system on the ATIP vehicles incorporates overhead sun shields to improve the quality of the point cloud data collected. Detection of overhead obstructions would require significant redesign of the LiDAR mounting arrangement and would adversely affect the quality of the data collected in the crossing. Therefore, the team was unable to accommodate this request.

Researchers proposed to store approximately 130 meters of data along the track (±65 meters from center of crossing) as a balance between longer scans that may be better suited to sightline analysis and the volume of data being transmitted through the cellular connection onboard the survey vehicle. Several stakeholders requested up to 1,000 meters of point cloud data at each crossing. An analysis of the file sizes associated with this length and the typical volume of data generated daily indicated that this would not be feasible using a cellular modem connection, particularly in rural areas with limited cellular signal bandwidth. Additionally, nearly eight times more cloud storage capacity along with the associated transmission bandwidth and processing capacity would be necessary to manage these scans.

3.1.3 Metadata

A stakeholder requested that the exact crossing angle be stored among the grade crossing metadata. Currently, the crossing angle is not calculated directly from the scan but queried from FRA's Grade Crossing Inventory which uses a 30° range (0°-29°, 30°-59°, 60°-90°). Calculating and storing the exact crossing angle is not within scope for the current task but could be addressed under a separate task in the future.

The Illinois Commerce Commission requested that the latitude and longitude of the middle of the crossing (as extracted from the LiDAR point cloud data) be stored. Currently, highway maintenance engineers and railroad employees rely on the Global Positioning System (GPS) location reported in FRA's Grade Crossing Inventory. This location information is provided by the submitting authority and could be derived from a low-resolution handheld GPS or estimated from available maps.

The LiDAR systems use the location reported by the Grade Crossing Inventory to trigger a geofenced data collection algorithm. This algorithm collects several hundred yards of data surrounding the reported crossing location, and additional data is collected to account for possible errors in the reported location. The point cloud data is then processed to identify the actual location of the grade crossing. After identifying the center of the crossing, the latitude and longitude associated with the highway-railway intersection is stored. Saving the detected grade crossing location will enable verification of location data submitted to FRA's Grade Crossing Inventory.

3.1.4 Planer Deviation Measurement

Previously, the grade crossing measurement algorithms calculated the planer deviation on both sides of the roadway and reported the larger magnitude measurement, storing the worst-case condition for a given grade crossing. Several stakeholders requested that the measured planer deviation on both sides of the roadway be stored to better characterize the condition of a given grade crossing and this requested capability was implemented.

3.2 Grade Crossing Algorithm Improvements

The initial version of the LiDAR Grade Crossing Inspection system was deployed to the DOTX220 survey vehicle in May 2019. A similar system was deployed onboard DOTX304, a hi-rail inspection vehicle, in December 2019.

Due to the significant variation in highway grade crossing configurations, the original effort focused on developing algorithms that were optimized for the most common types of crossings encountered. According to information obtained from FRA's Grade Crossing Inventory, the most common grade crossing configuration is a single track crossing the highway at an angle between 60° and 90°. Of the grade crossings that reported crossing angle information, 79.7 percent fall into this category. Similarly, 71.4 percent of crossings that reported the number of tracks were single-track crossings.

The developed algorithm accurately measured the planer deviation at grade crossings similar to the common configuration, namely single-track crossings intersecting the roadway at close to 90° (Figure 8). After reviewing a selection of crossings with high reported planer deviation values and manually verifying the roadway profile, the team discovered that inaccurate planer deviation measurement could be classified into three groups: uncontrollable environmental factors, sharp intersection angles between the roadway and track, and the presence of vegetation or structures near the crossing.

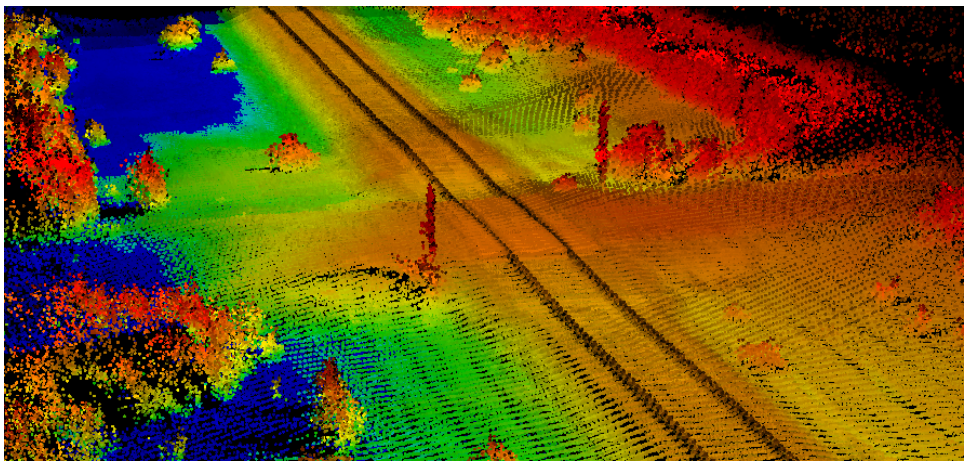

Figure 8: A simple grade crossing with a single-main track and approximately perpendicular roadway intersection angle

3.2.1 Examples of Challenging Crossings

Uncontrollable factors such as other rail traffic, maintenance-of-way, or roadway construction equipment occasionally can occupy a crossing while the point cloud is being collected (Figure

9). This results in inconsistencies in the roadway surfaces being analyzed by the algorithm and adversely influences the resulting planer deviation measurement. These results accounted for approximately 5 percent of incorrectly identified high-planer deviation crossings under review.

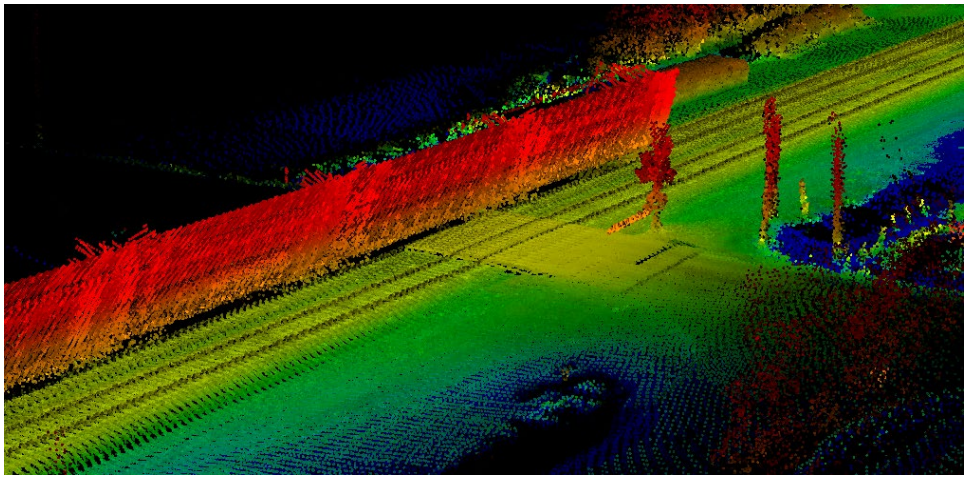

Figure 9: A double-track grade crossing with other rail traffic occupying the adjacent track

Occasional errors in FRA's Grade Crossing Inventory, which serves as an input to the geofenced data collection system, can result in grade crossing point clouds being collected at locations without a crossing, locations with a closed or removed crossing, or at an above or below grade crossing (Figure 10). Results obtained from the algorithm under these conditions are not relevant to the identification of humped grade crossings. These conditions accounted for approximately 10 percent of the erroneous high-planer deviation sites under review.

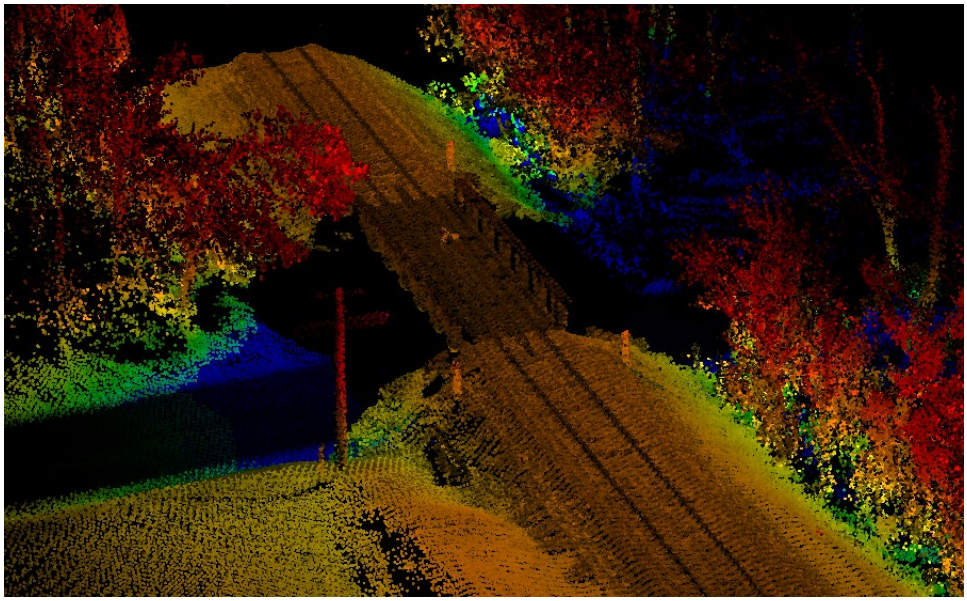

Figure 10: An "above-grade" crossing erroneously reported in FRA's Grade Crossing Inventory as "at-grade"

Additionally, conditions related to the configuration of the crossing accounted for approximately 85 percent of the high-planer deviation sites under review. Several conditions fall into this category, including two or more tracks in the crossing, which occasionally are not detected and correctly represented in the measurement algorithm (Figure 11). In cases such as this, the required nine meter lateral offset distance from each rail will include part of the adjacent track, resulting in a measurement point that is not consistent with the AASHTO standard.

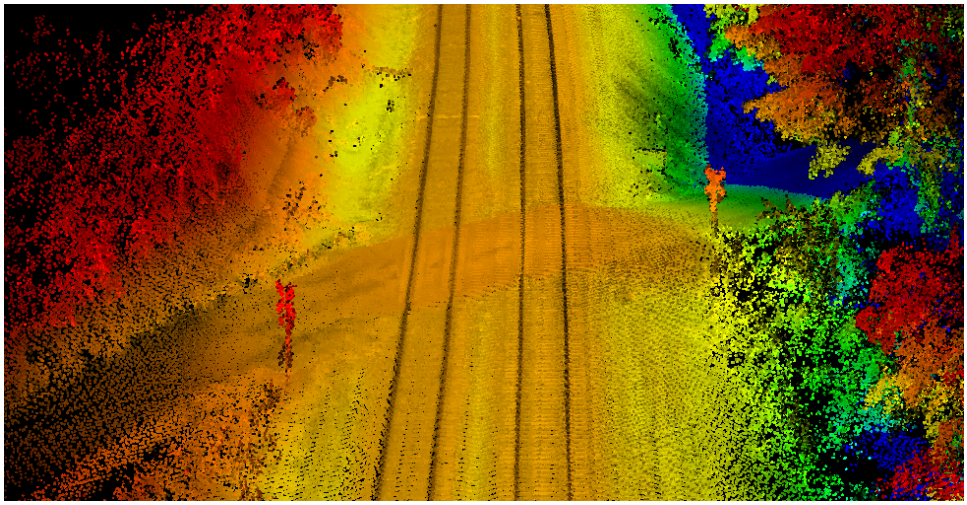

Figure 11: A double-track grade crossing with a sharp intersection angle between the roadway and track

Sharp intersection angles between the roadway and track were significant contributors to incorrectly identified high-planer deviation sites (Figure 12). The existing algorithm was optimized for performance on crossings with near-perpendicular roadway intersections. While analyzing crossings with a sharp roadway intersection, the algorithm often does not accurately identify the change in roadway position and adjust the search area used to measure planer deviation.

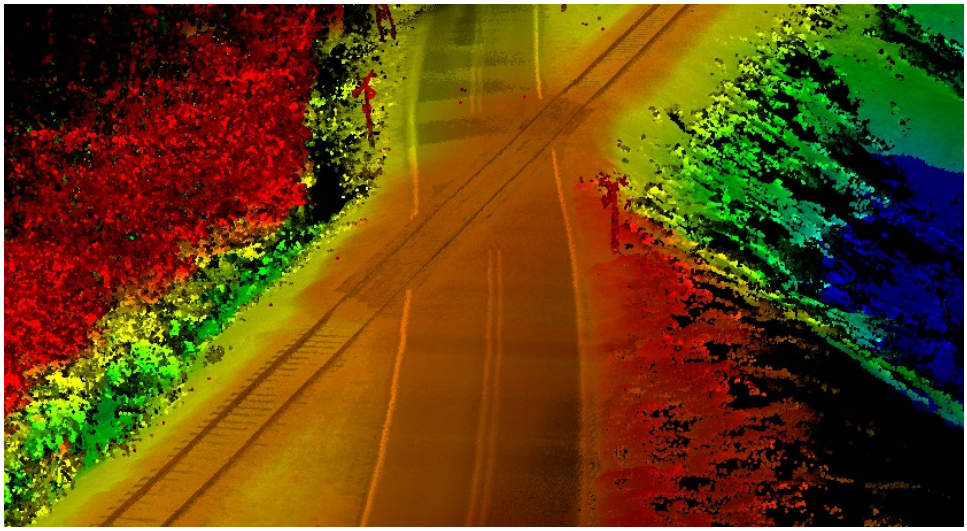

Figure 12: A single-main grade crossing with a sharp intersection angle between the roadway and track

3.2.2 Algorithm Improvements

Once the conditions that lead to inaccurate planer deviation measurements were better understood, the team implemented a plan to optimize performance of the algorithms under these conditions. The team first removed small to medium size objects such as vegetation, signage and crossing gates, and motor vehicles from the point cloud data (Figure 13).

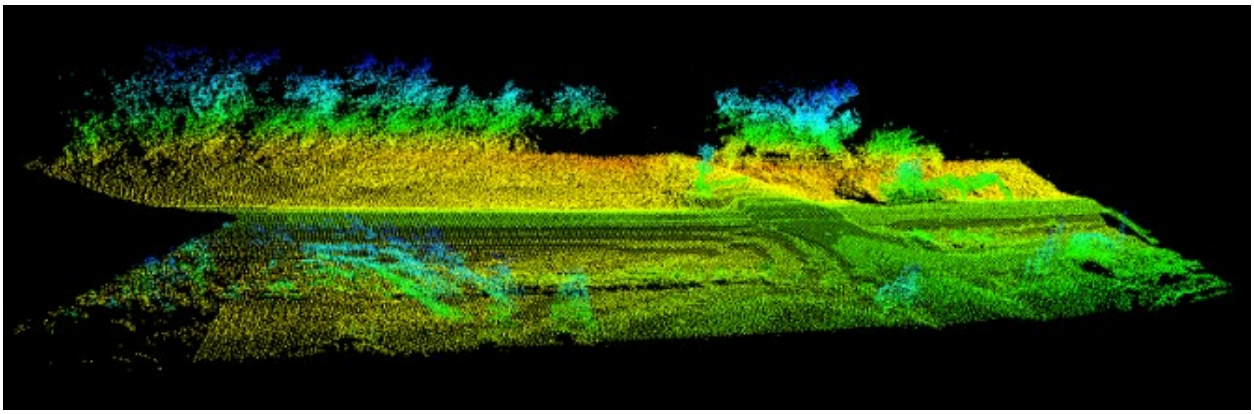

Figure 13: Initial point cloud scene collected using LiDAR scanner array

A Progressive Morphological Filter (PMF) was implemented to remove points on the boundaries of objects within the point cloud. The points selected for removal were based on the algorithm's window size, with objects larger than the window size being preserved. The filter was applied repeatedly with progressively larger window sizes. This approach progressively smooths irregularities such as vegetation, signage, and other objects present in the point cloud while leaving planer surfaces largely unaffected (Figure 14).

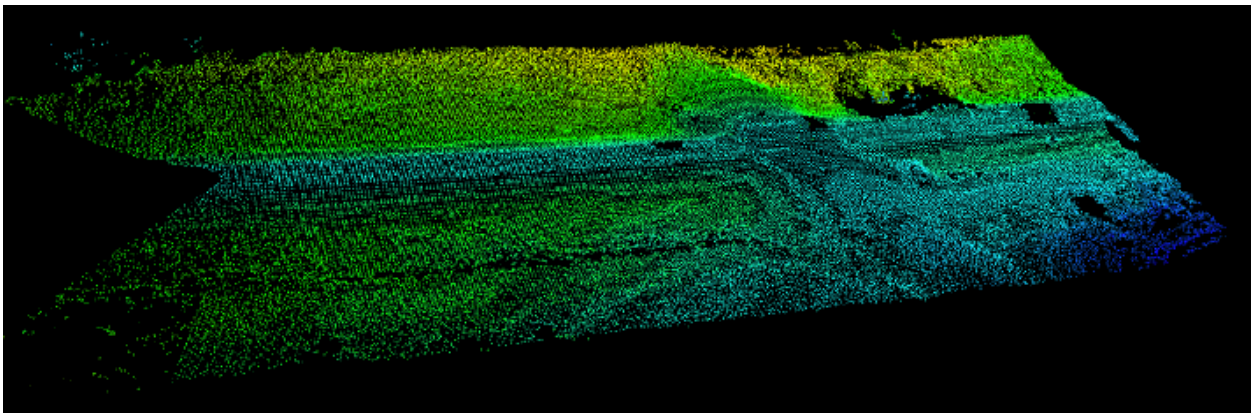

Figure 14: Scene after successive applications of Progressive Morphological Filter

The team then fit the plane to the ground using Support Vector Machines (SVM), and any points that resided on this plane were removed. After this step, only points registered on raised and lowered surfaces remained. This includes the tracks and intersection if there was an incline leading up to the track. The remaining surface in the point cloud will have gaps where the ground level data was removed (note the black voids shown in Figure 15).

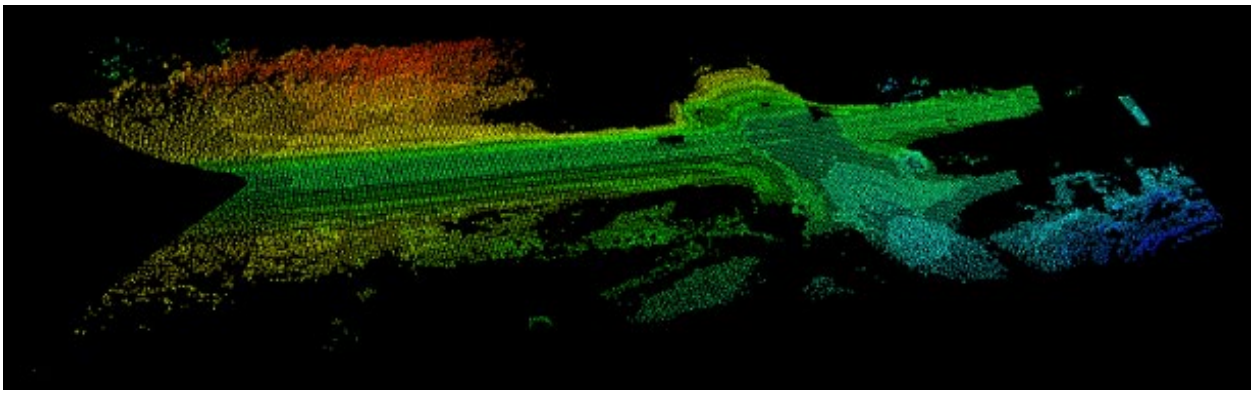

Figure 15: Scene after Support Vector Machine plane fitting to identify ground level

After removal of vegetation, signage, motor vehicles, and other objects not part of the roadway and tracks, the normal vectors were calculated for each point in the point cloud. The normal vectors characterize the orientation of the surfaces that each point lies on, specifically the direction represented by x, y, and z components. The resulting region of interest is the initial segmentation of the track and roadway as shown in the left side of Figure 16.

K-Means clustering was then used to group points surrounding this region of interest, followed by a linear SVM to identify a line that separates points on the roadway well (right side of Figure 16). This line represents the best fit for the centerline of the roadway based on the segmented surfaces and was plotted as a blue line on an overlay image (right side of Figure 16).

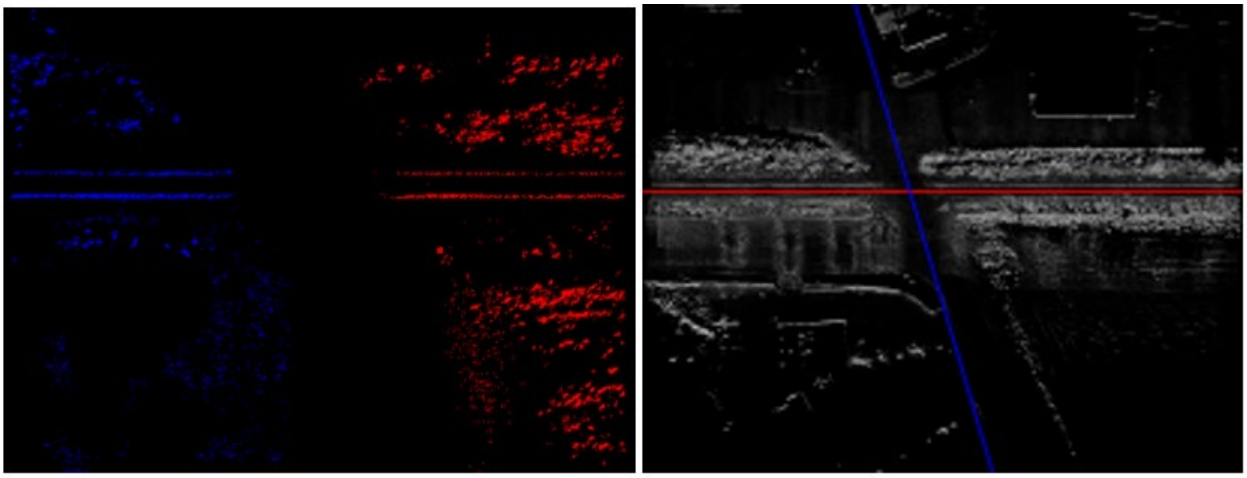

Figure 16: Scene after SVM segmentation (left) and Linear SVM (right)

Checks are in place to ensure the line generated by the SVM is plausible, and a correction mechanism will attempt to re-estimate the line if necessary (see "*road_line"* variable in Figure 17 below).

The LiDAR scanner array and the vehicle's onboard Inertial Measurement Unit (IMU) and GPS sensor package were used to identify the center of the survey vehicle's track. The point cloud's coordinate system was shifted to align with the identified track centerline. The track center x, y, and z coordinates at this point were stored and the track used by the survey vehicle was plotted on an overlay image as a red line (right side of Figure 16).

Next, detection of adjacent tracks was performed, and their coordinates saved if detected. A k-dimensional tree search was performed between the track centerline coordinates and the roadway surface to identify locations where the planer deviation is to be calculated. This search was performed at an offset of nine meters on both sides of the survey vehicle's track, or in the case of multiple tracks, nine meters from the first and last tracks in the crossing. The resulting locations within the roadway (denoted *"Y_search"* in Figure 17) were used to calculate the largest difference in elevation on either side of the crossing. The maximum elevation found within the search locations, along with the coordinates where the maximum is located, were stored in the *"Y_search_max"* variable. The results from both sides of the crossing were stored and the larger of the two was reported as the planer deviation of the crossing. The *"Y_search_max"* results were then plotted as green dots on an overlay image and saved as shown in Figure 17.

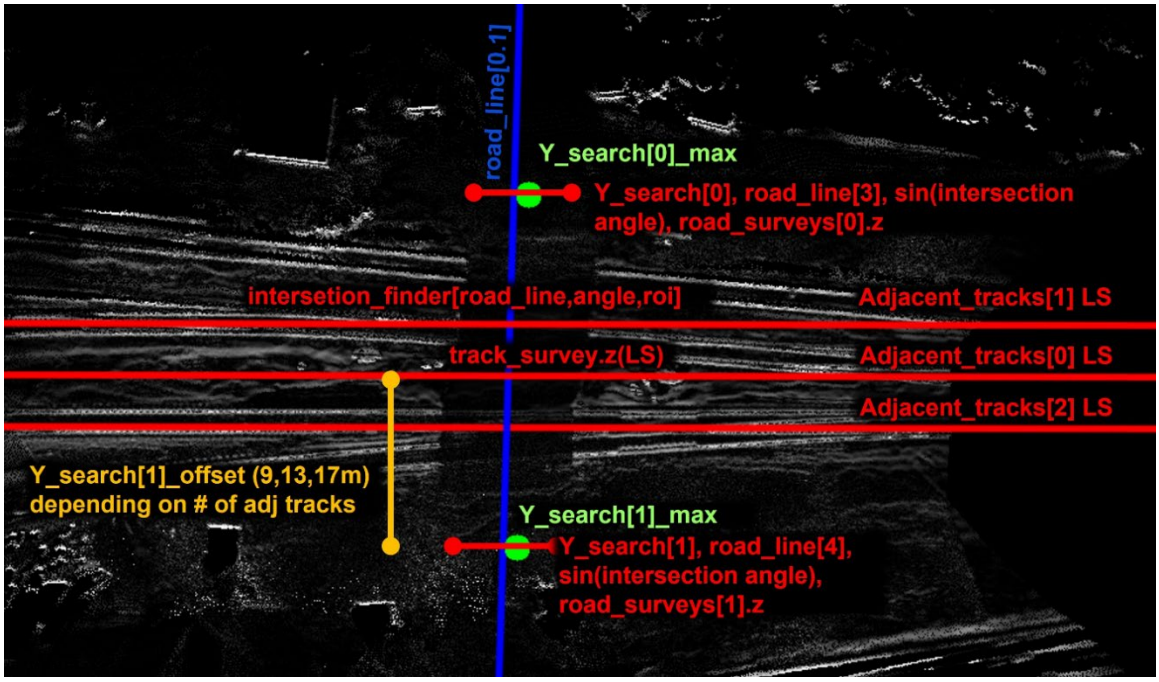

Figure 17: Grade crossing scene after SVM segmentation annotated with search algorithm variables

After performing the SVM segmentation, the quality of the roadway surface separation can be calculated based on the number of outlier points and their distance from the fitted centerline. Because the quality of the roadway separation and resulting estimation of roadway centerline is critical to the accuracy of the planer deviation measurement, this calculated value functions as a measure of confidence for the resultant algorithm outputs.

Paved, hard surface roadways, such as concrete and asphalt, with close to perpendicular intersection angles will achieve close to 100 percent segmentation confidence (see Figure 16 above). Hard surface, paved roadways with intersection angles less than 60° will result in greater than 80 percent segmentation confidence, while gravel surface roadways will result in 50 percent or higher segmentation confidence.

Unpaved dirt roads, common at farm crossings, often have vegetation growing in the roadway to a height of 0.5 – 1 meter. When the roadway vegetation has a similar height and surface texture compared to the surrounding areas, the roadway surface often blends in with the rest of the

surrounding vegetation. When this occurs, the algorithm will often report segmentation confidence of approximately 30 percent. Figure 18 shows a heavily vegetated farm crossing. Although the algorithm did correctly identify locations within the roadway for measurement of the planer deviation, the PMF was unable to effectively smooth all vegetation from the roadway. This resulted in inaccurate planer deviation measurements because the elevation of the remaining vegetation was included in the reported measurement.

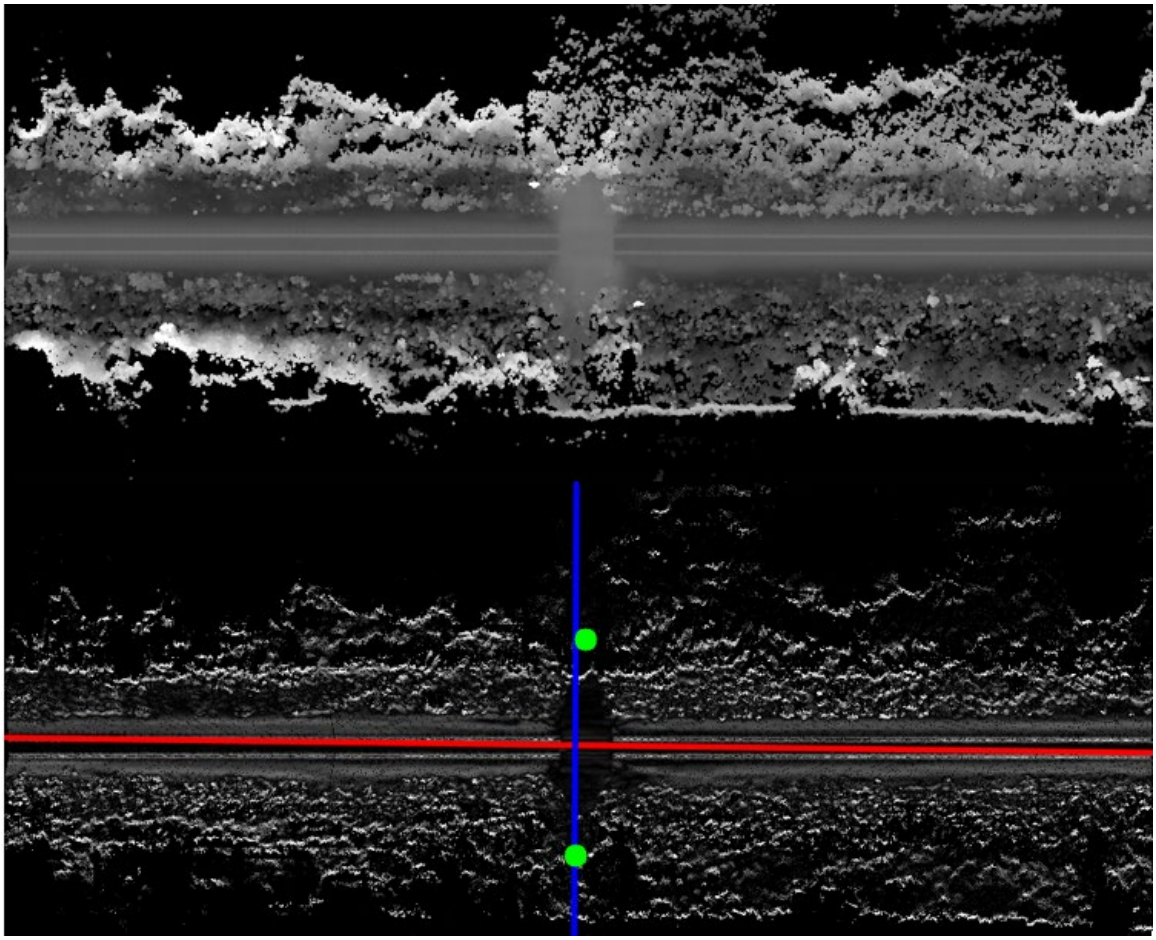

Figure 18: Unpaved farm crossing with approximately 0.5 - 1m vegetation resulting in 30 percent confidence

Lastly, in cases where FRA's Grade Crossing Inventory provides an erroneous GPS location for a crossing, data will be collected that does not include any roadways or crossings (Figure 19). In these situations, the algorithm will often fail to converge on a location, although occasionally a slightly smoother surface may be identified as a roadway and a planer deviation value reported.

The track and roadway centerlines plotted in the overlay images can be used to estimate the crossing intersection angle. In cases where the roadway is well defined and the algorithm produces a result with a high confidence value, the calculated intersection angle is representative of the true layout. However, due to variations in the roadway surfaces, the fitted centerline may be off by 10 degrees of more while still producing accurate planer deviation measurements. Considering this behavior, use of the calculated intersection angle measurement should only be used when algorithm confidence approaches 100 percent.

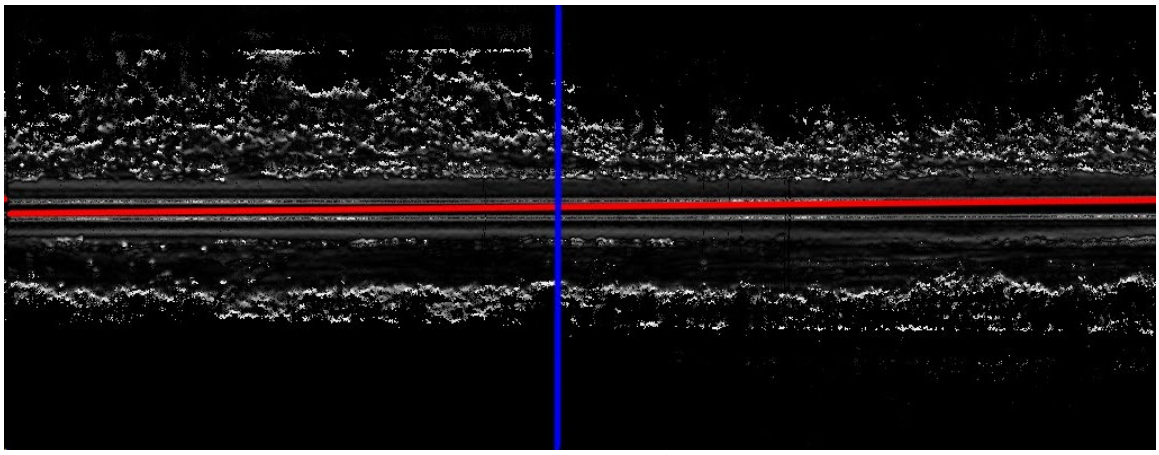

Figure 19: Point cloud processed at a location without a crossing resulting in 23 percent segmentation confidence

3.3 Data Transfer and Storage

The original data flow was composed of a manual data transfer off the ATIP collection vehicle via external hard drive, followed by post-processing of the data on a local workstation (Figure 20). This process was labor intensive and resulted in delayed access to the collected crossing scans and resulting measurements.

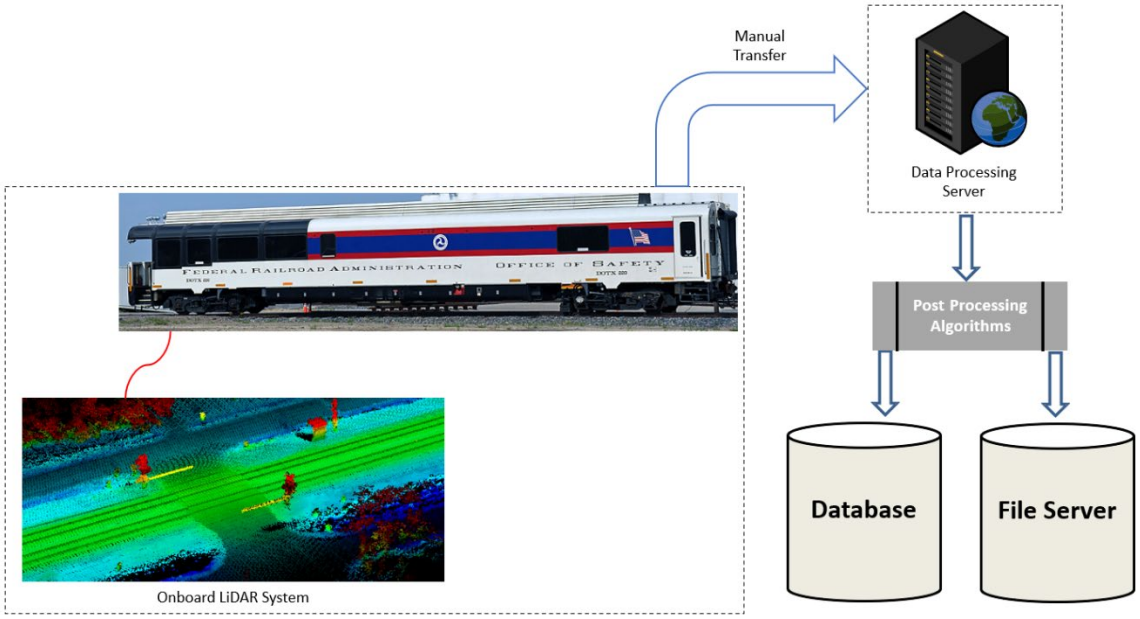

Figure 20: Schematic showing data flow with manual offloading

To streamline the data workflow, the post processing routines were integrated into the on-board data collection software (Figure 21). This allowed for ongoing collection of grade crossing data with lower labor costs, while reducing the time required to access and review new grade crossing data. To implement this updated data workflow, the post-processing algorithms were integrated into the geofencing and data collection software onboard the ATIP vehicles.

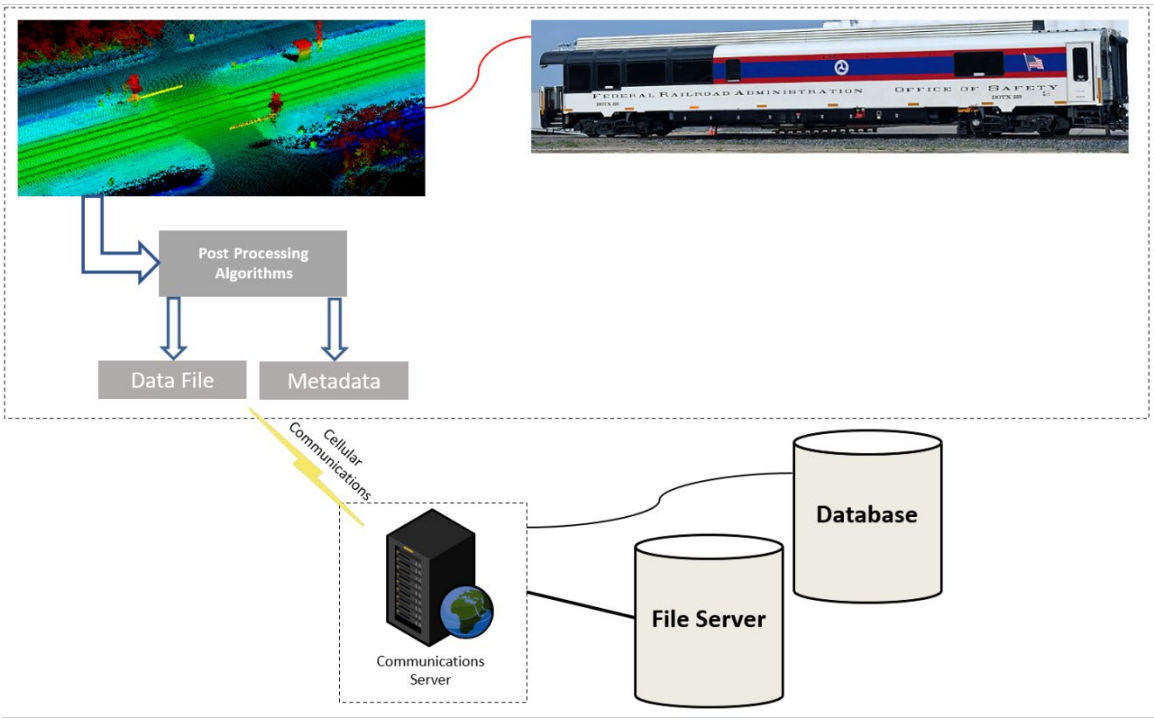

Figure 21: Schematic showing updated data flow with onboard processing and cellular transfer

3.4 Other Methods of Grade Crossing Inspection

The use of ATIP survey vehicles as a collection platform for LiDAR grade crossing data was very successful. The LiDAR equipped ATIP vehicles conduct survey operations most of the year and together inspect between 22,000 and 25,000 miles of track in the United States every year. Installation of an autonomous measurement system onboard the vehicles leverages the existing track coverage under the ATIP program and has minimal impact to survey operations. Similarly, the cost to maintain the system and continue data collection efforts is minimal.

ATIP vehicles have proved to be an effective platform to survey grade crossings in the United States. However, due to the routing of ATIP vehicles and the priority to survey more heavily used, mainline routes, not all crossings are on routes that will be surveyed by ATIP. Considering this, FRA is evaluating other means of collecting 3-D point cloud data at grade crossings.

4 Analysis & Algorithm Validation

Throughout the algorithm development efforts, researchers used an iterative process to gauge improvements in the planer deviation measurements by evaluating a sample set of crossing scans with several challenging characteristics. After optimizing algorithm performance, a more comprehensive assessment of the measurement accuracy was undertaken to validate the changes. An analysis of the distribution of planer deviation measurement with respect to relevant crossing parameters was performed, as well as a coverage analysis to determine whether ATIP vehicle routing produced a representative sampling of grade crossings in the United States.

4.1 Algorithm Validation

The set of all grade crossing scans was divided into subsets based on the following relevant characteristics:

- High planer deviation – crossings with more than 1 meter of planer deviation as reported by the analysis algorithms
- Significant change in planer deviation – crossings that were scanned and processed with the original algorithms and subsequently reported a change in planer deviation greater than 0.25 meter
- Sharp intersection angle – crossings that were reported with a roadway intersection angle less than 40°
- Random sampling – a selection of crossings falling outside the categories above

A total of 85 crossings were randomly selected from each of the 4 categories above, with the individual count from each category selected to approximately match the overall prevalence within the dataset (Table 2). These crossings were manually reviewed, and planer deviation measurements taken for comparison to the algorithm outputs.

Table 2: Number of algorithm validation samples selected and respective categories

Selection Criteria	Number of Samples
High Planer Deviation	15
Change in Planer Deviation	30
Sharp Intersection Angle	20
Random Selection	20

The manual review process for each scan consisted of two steps. First, the team visually reviewed the Bird's-Eye-View (BEV) overhead image that is generated after processing each crossing scan (Figure 22). This image is annotated to show the track traversed by the survey vehicle and any adjacent tracks in red. The roadway segmentation line is shown in blue. The locations identified with maximum planer deviation on either side of the crossing are marked with green dots. This image provides a confirmation that the critical locations needed for accurate determination of planer deviation were identified correctly.

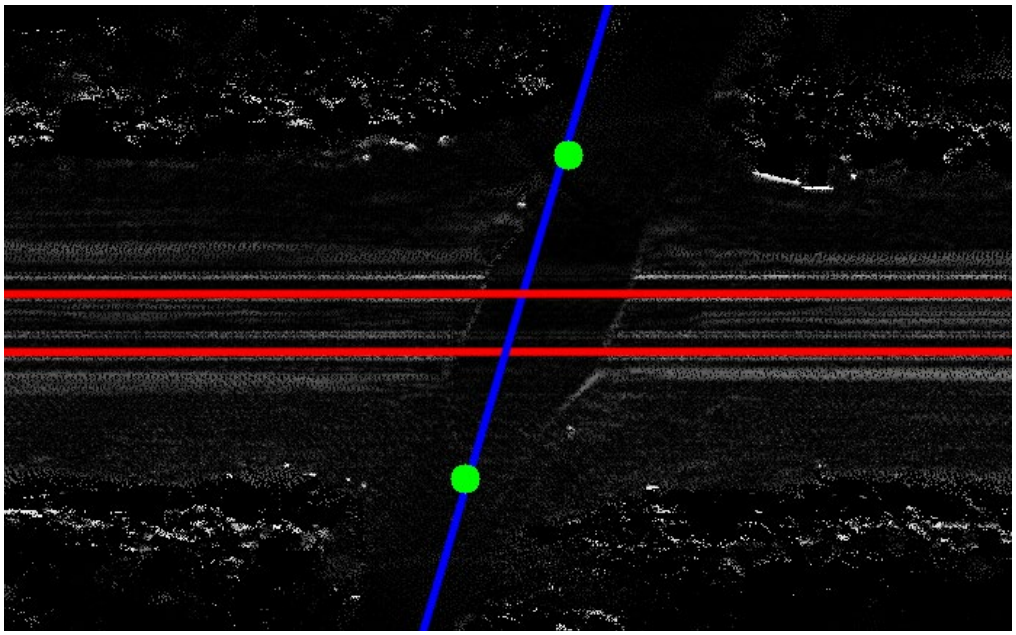

Figure 22: Example of Bird's-Eye-View image generated for each crossing

Second, a point cloud viewer was used to review the crossing scan and take manual planer deviation measurements (Figure 23). The point cloud is color coded based on elevation, providing a visual indication of height and gradient of surfaces within the scan. The viewer allows for 3D rotation of the point cloud, can display the coordinates of individual points with the cloud, and can take relative measurements in one, two, or three dimensions. These capabilities allowed the researchers to precisely measure lateral offsets from both rails, ensuring compliance with AASHTO standards. Once the correct locations with the roadway had been identified, determination of the roadway elevation relative to the top of rails was measured. After manually measuring the planer deviation on both sides of the crossing, the values were saved for later analysis.

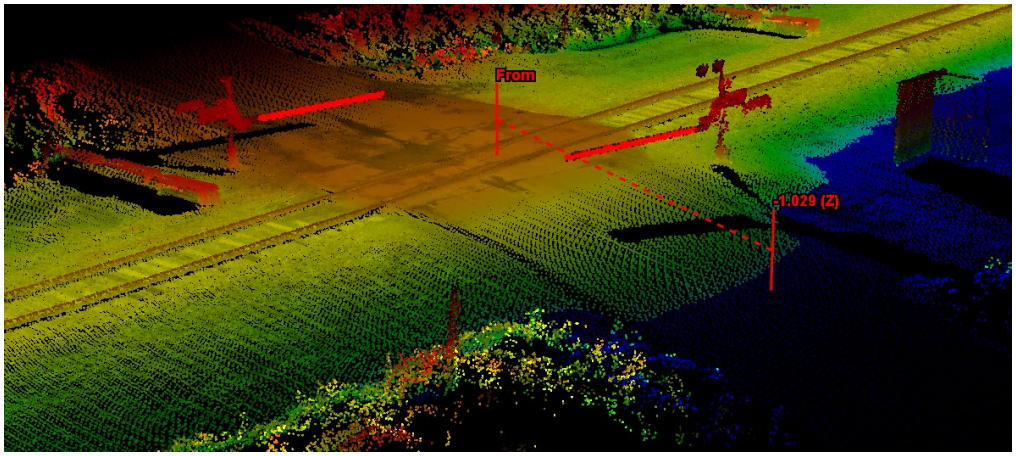

Figure 23: Example crossing showing relative elevation measurement used to manually confirm planer deviation reported by the algorithm

4.1.1 High Planer Deviation Crossings

Crossings with a reported planer deviation value greater than 1 meter are among the steepest roadway approaches surveyed by the ATIP LiDAR equipped vehicles, representing only 7.2 percent of all crossings scanned to date. Fifteen crossings were selected from this category for manual review. The manual measurements were compared to the algorithm outputs for each of the 15 crossings and the differences are shown in Figure 24.

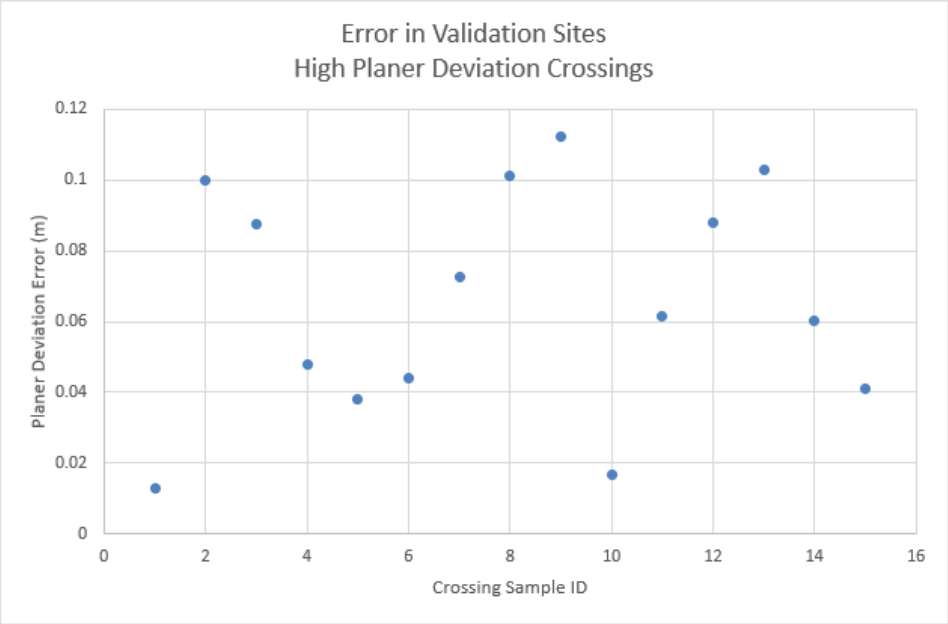

Figure 24: Error in algorithm outputs at 15 high planer deviation crossings

The error varied from a minimum of 0.013 meter to a maximum of 0.112 meter, with a median error of 0.061. Additional statistics are provided in Table 3.

Table 3: Algorithm validation statistics for high planer deviation crossings

Criteria	Difference (m)
Min	0.013
25%	0.042
Median	0.061
75%	0.094
Max	0.112
STD	0.032

The largest error found during validation of high planer deviation sites occurred at crossing 051014X. This is a complex crossing with two approaching roadways on one side of the crossing. The location identified by the algorithm is in the median between two roadways, a location unlikely to be traversed by a motor vehicle (upper green dot in Figure 25).

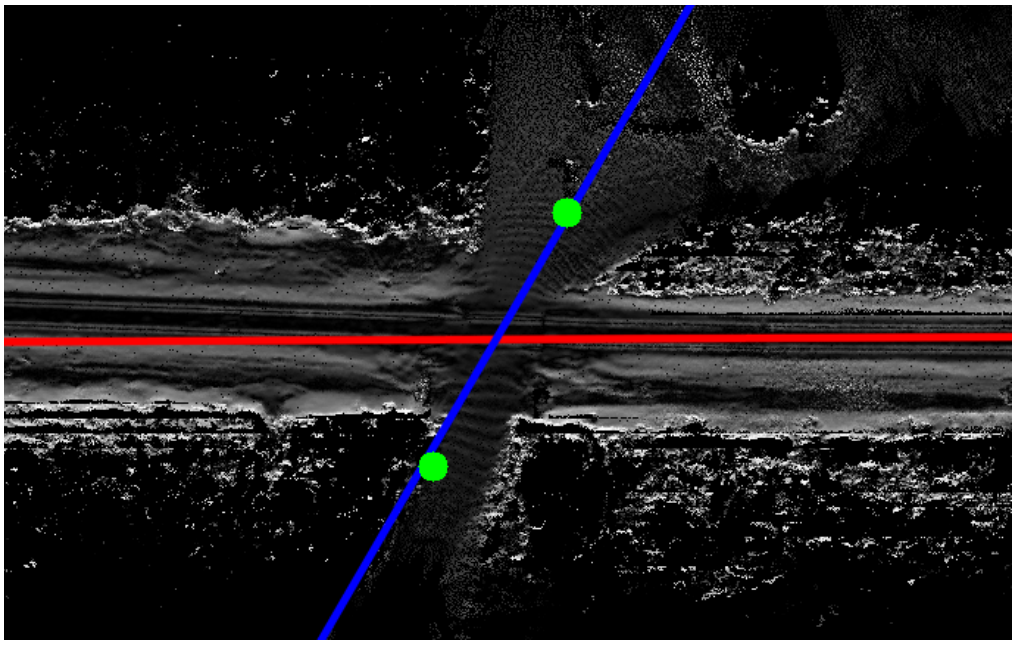

Figure 25: Bird's-Eye-View of crossing 051014X showing identified maximum planer deviation on both sides of track

Shown below are 3D views of crossing 051014X (Figure 26 and Figure 27). The approaching roadway on the upper right side of Figure 25 has the steepest gradient and would correspond to the largest planer deviation if it were the primary roadway. The location identified by the algorithm is located between the two approaching roadways and the corresponding planer deviation value falls between the correct value for the respective roadways.

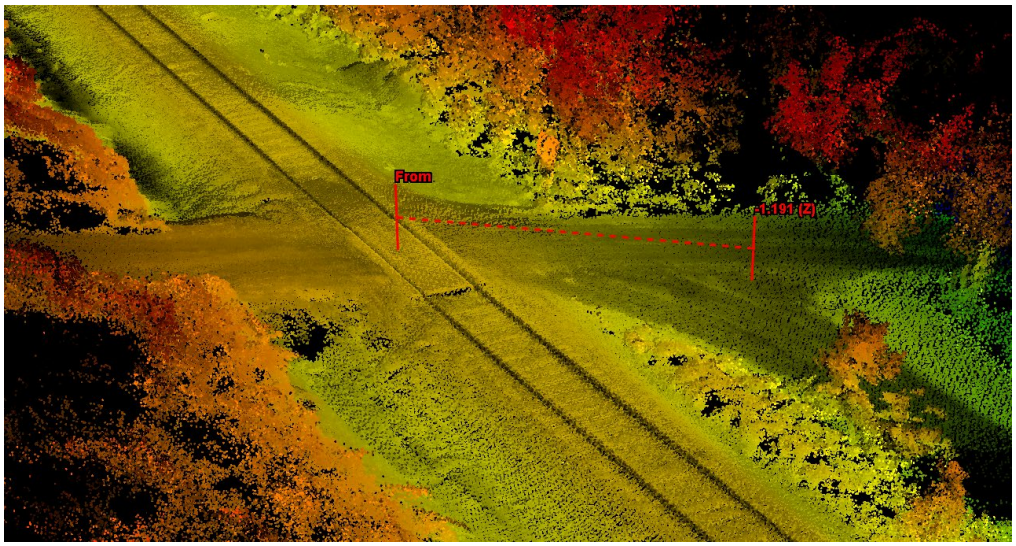

Figure 26: Point cloud view of crossing 051014X showing identified maximum planer deviation

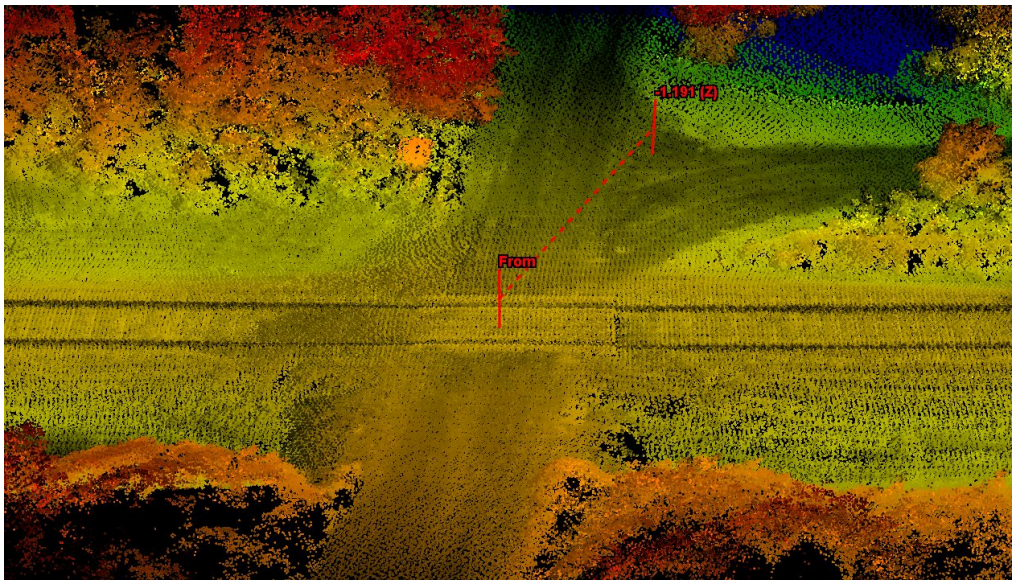

Figure 27: Alternate view of crossing 051014X showing identified maximum planer deviation

4.1.2 Crossings with Large Change in Reprocessed Planer Deviation

After reprocessing the original dataset collected between May 2019 and September 2020, the team compared outputs from the original and updated algorithms to validate the accuracy of the updated algorithm outputs. Thirty crossings were randomly selected from the subset of locations with a reported change in planer deviation of greater than 0.25 meter. Manual measurements of planer deviation were compiled and compared to the algorithm outputs for each of the 30 crossings. The differences for each crossing are shown in Figure 28.

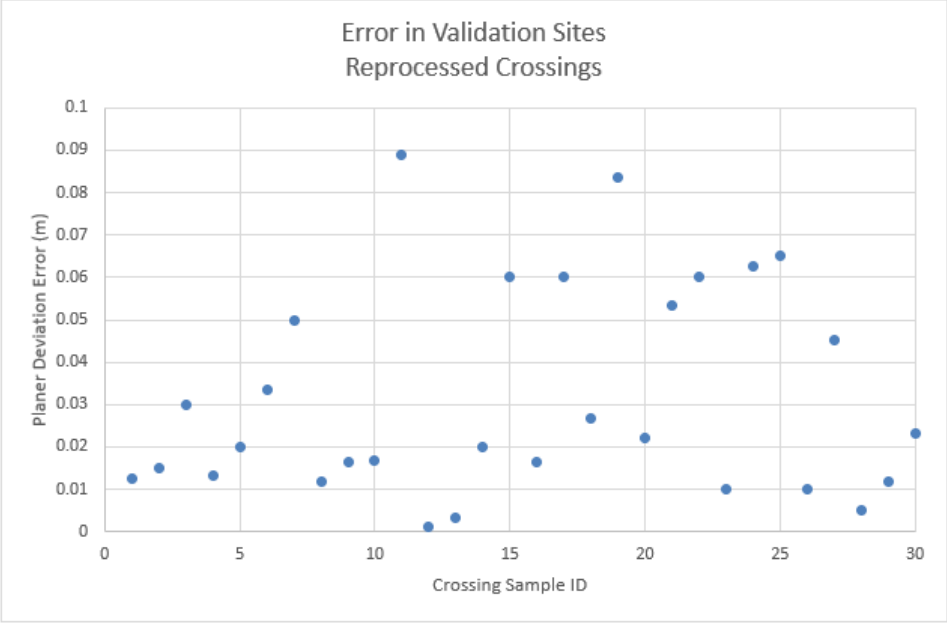

Figure 28: Error in algorithm output at reprocessed crossings with greater than 0.25-meter change in planer deviation

The error varied from a minimum of 0.001 meter to a maximum of 0.089 meter, with a median error of 0.021 meter. Additional statistics are provided in Table 4.

Table 4: Algorithm validation statistics for locations with a change in reported planer deviations greater than 0.25-meter

Criteria	Difference (m)
Min	0.001
25%	0.013
Median	0.021
75%	0.053
Max	0.089
STD	0.025

The largest error found during validation occurred at crossing 732405Y. This is a complex crossing with a paved road intersecting the tracks at approximately 45° and a secondary road that parallels the track and merges at the crossing (Figure 29).

Figure 29: Satellite imagery showing crossing 732405Y

The location identified by the algorithm is in the unpaved portion of the road that parallels the track, in a location that could be occupied by a long-wheelbase vehicle based on the roadway approach angles and clearances (upper green dot in Figure 30).

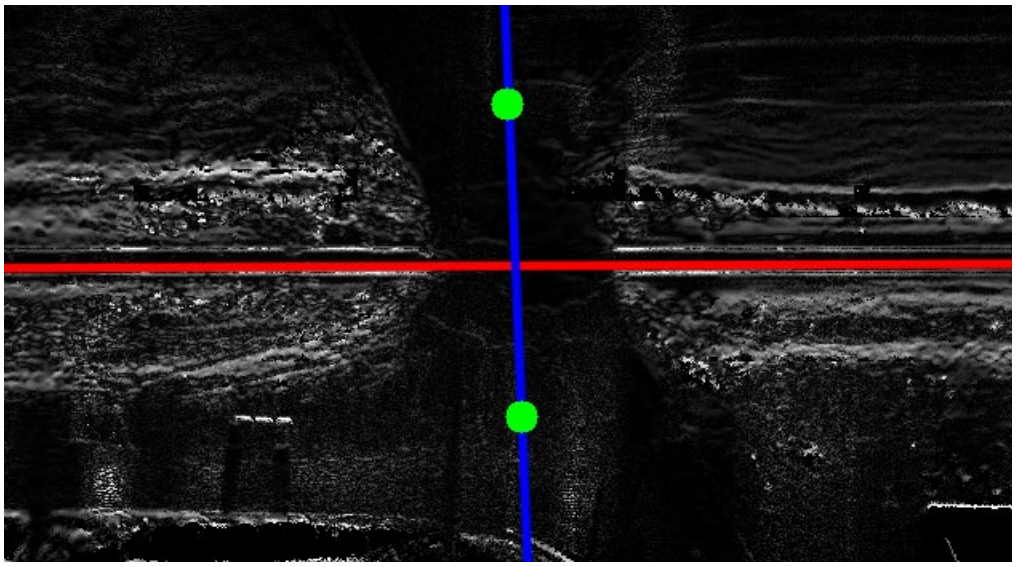

Figure 30: Bird's-Eye-View of crossing 732405Y showing identified maximum planer deviation on both sides of track

Shown below is a 3D view of crossing 732405Y (Figure 31). The site corresponding to the maximum identified planer deviation falls outside of the paved primary approach road, although it would be possible for a vehicle to occupy this location.

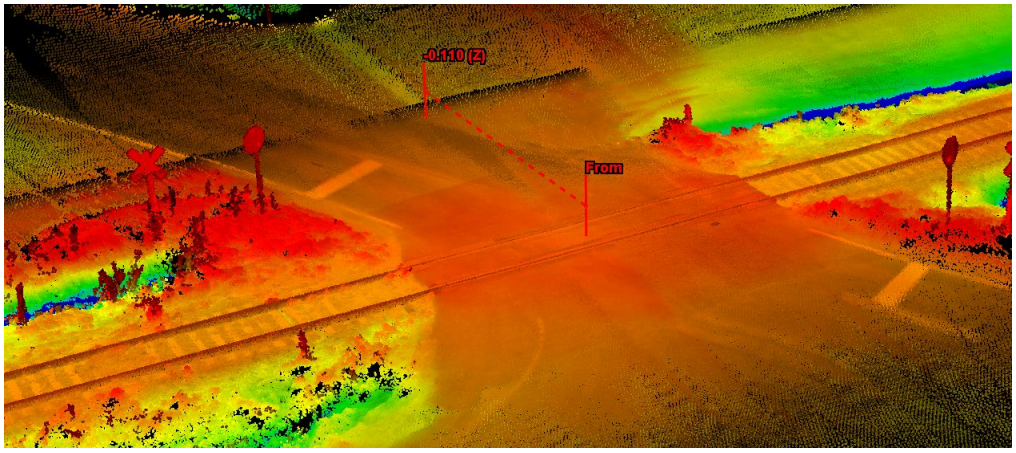

Figure 31: Point cloud view of crossing 732405Y showing identified maximum planer deviation

4.1.3 Sharp Roadway Intersection Angle

Validation of algorithm performance when analyzing grade crossings with sharp intersection angles is particularly important. Incorrect identification of the roadway surface can result in the reported planer deviation value being measured outside of the roadway, in a drainage ditch, or in adjacent vegetation, significantly reducing accuracy. Additionally, this crossing configuration was particularly challenging for the original analysis algorithm, becoming a critical aspect of improving algorithm performance. Twenty grade crossings with a roadway intersection angle less than 40 degrees were selected from the dataset. The crossing intersection angle reported by the algorithm was used to select the validation sites. The values listed in FRA's Grade Crossing

Inventory are grouped into bins of 30° intersection angles and are not sufficiently precise for this analysis. Following manual determination of the planer deviation, the difference from the reported value was calculated (shown below in Figure 32). Note that two of the randomly selected crossings had been closed and removed prior to data collection. These crossings had paved surfaces adjacent to the track which were identified as the roadway, leading the algorithm to identify the surfaces as a roadway crossing at a sharp intersection angle. Because there is no roadway to which to compare for a manual measurement, these crossings were not included in the error statistics provided below.

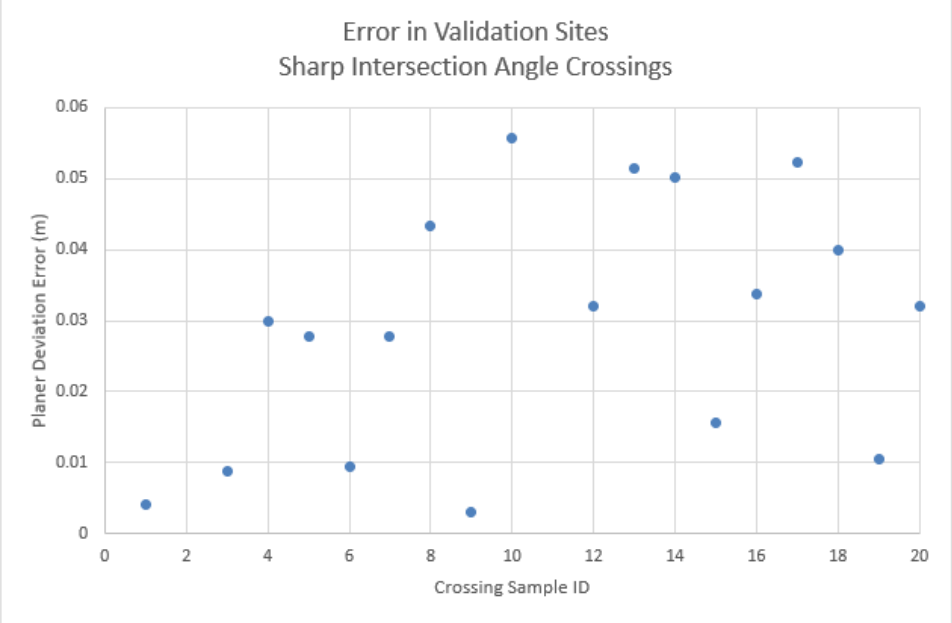

Figure 32: Error in planer deviation reported at sharp intersection angle validation sites

The error varied from a minimum of 0.003 meter to a maximum of 0.056 meter, with a median error of 0.030 meter. Additional statistics are provided in Table 5.

Table 5: Algorithm validation statistics for locations with roadway intersection angle less than 40 degrees

Criteria	Difference (m)
Min	0.003
25%	0.010
Median	0.030
75%	0.041
Max	0.056
STD	0.018

The largest error found during validation of locations with sharp intersection angle occurred at crossing 847210G. This crossing includes a curved roadway intersecting a single main track (Figure 33).

Figure 33: Satellite imagery showing crossing 847210G

The location identified as having the greatest planer deviation by the algorithm is near the inside shoulder of the curved roadway (top right in Figure 34).

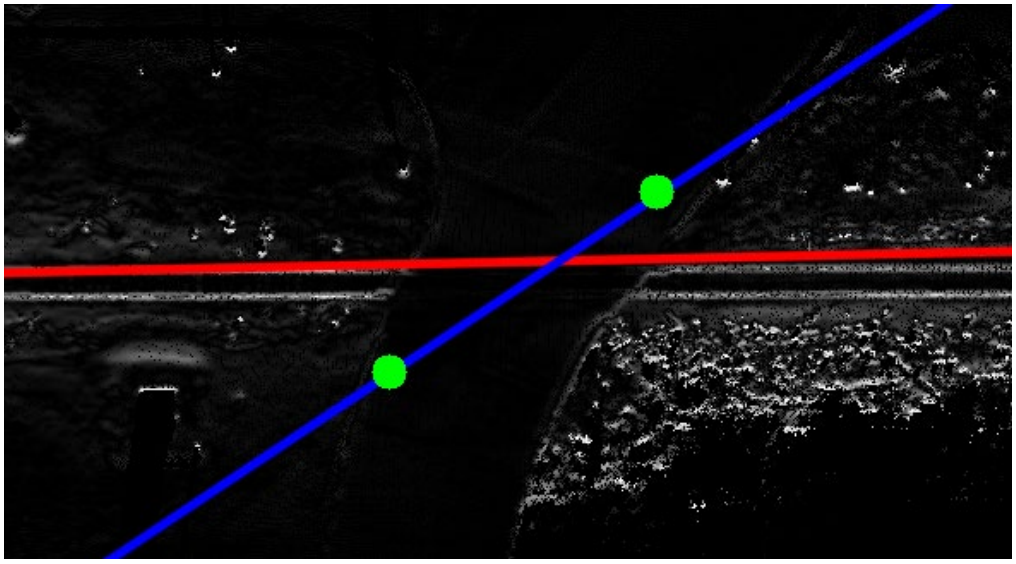

Figure 34: Bird's-Eye-View of crossing 847210G showing identified maximum planer deviation on both sides of track

The curvature of the roadway, specifically the differing curvature on opposite sides of the crossing, resulted in the algorithm segmenting the roadway using a fit that includes a sharper intersection angle than is correct. The calculated intersection angle is used to adjust the lateral offset for non-perpendicular crossings. In this case the offset was not large enough due to the incorrect angle approximation.

Shown below is a 3D view of crossing 847210G (Figure 35). The site corresponding to the maximum identified planer deviation falls outside of the paved primary approach road, although it would be possible for a vehicle to occupy this location. Despite the error in the crossing angle calculation, the effect on the reported planer deviation was minor because there was very little vertical profile within the roadway.

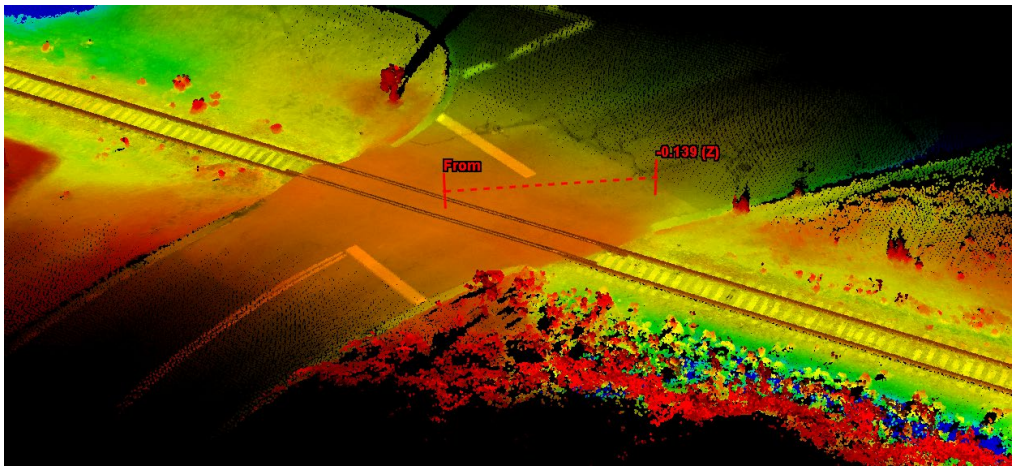

Figure 35: Point cloud view of crossing 847210G showing identified maximum planer deviation

4.1.4 Random Selection

The last group of locations used for algorithm validation were randomly selected from the remaining crossings in the dataset. Twenty crossings were selected outside of the categories listed above, intended to give a random sampling of the more common crossing configuration, specifically, moderate intersection angle and planer deviation. The manual measurements were compared to the algorithm outputs for each of the 15 crossings and the differences are shown in Figure 36.

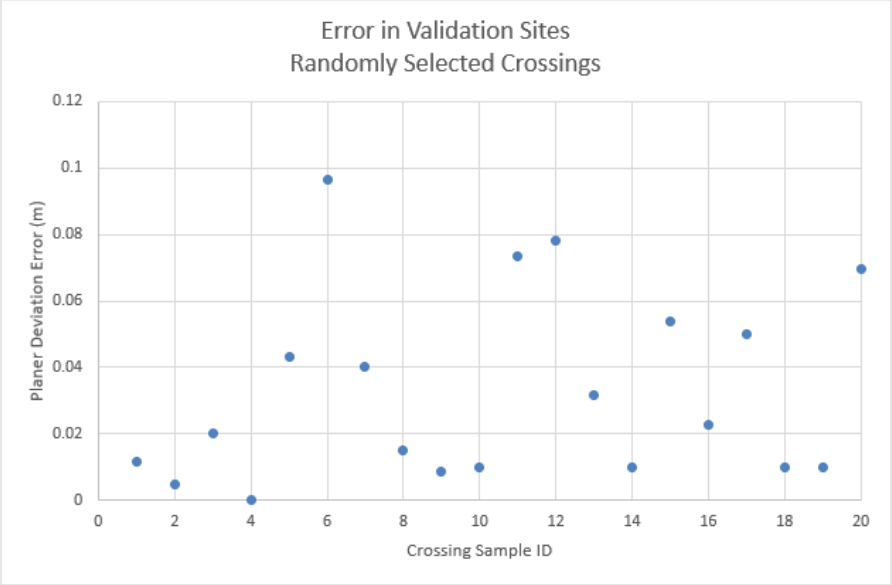

Figure 36: Error in algorithm outputs at 20 randomly selected crossings

The error varied from a minimum of 0 meter to a maximum of 0.097 meter, with a median error of 0.021 meter. Additional statistics are provided in Table 6.

Table 6: Algorithm validation statistics for randomly selected crossings

Criteria	Difference (m)
Min	0.000
25%	0.010
Median	0.021
75%	0.051
Max	0.097
STD	0.029

The largest error found during validation of randomly sampled sites occurred at crossing 304510V. This is a single main crossing with an intersection angle of approximately 60 degrees. The algorithm incorrectly identified a second track, resulting in an incorrect offset distance used to calculate the planer deviation.

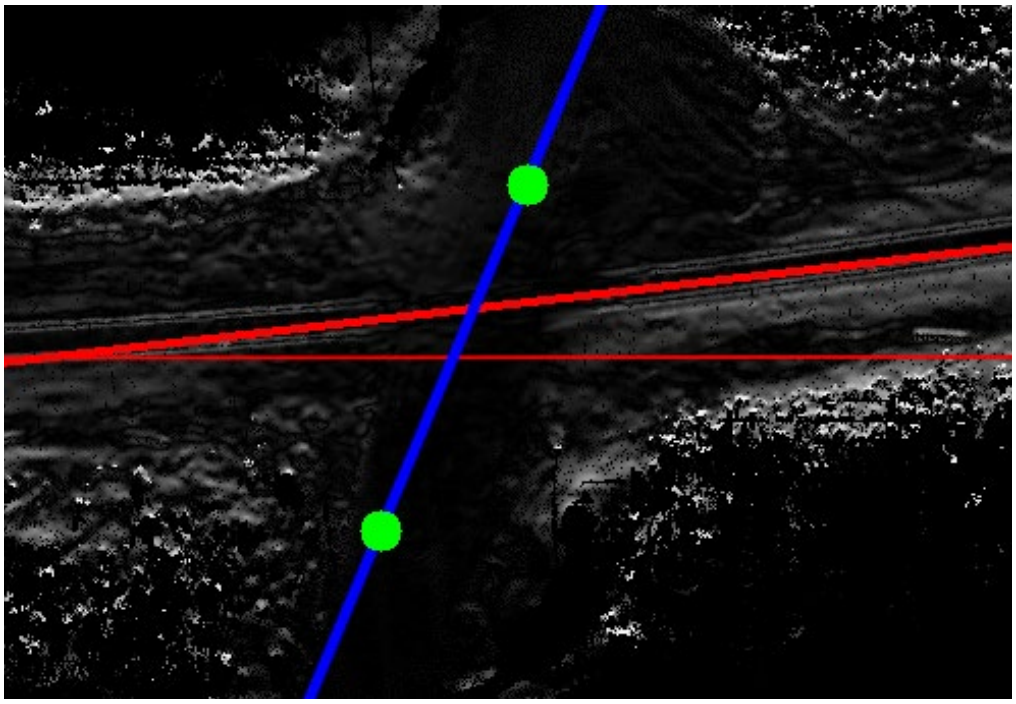

Figure 37: Bird's-Eye-View of crossing 304510V showing identified maximum planer deviation on both sides of track

Shown below is a 3D view of crossing 304510V (Figure 38). The location associated with the maximum planer deviation does lie within the roadway and the intersection angle was accurately estimated by the algorithm. The erroneous identification of a second track affected the offset distance used, resulting in a slight reduction of the magnitude of maximum reported planer deviation.

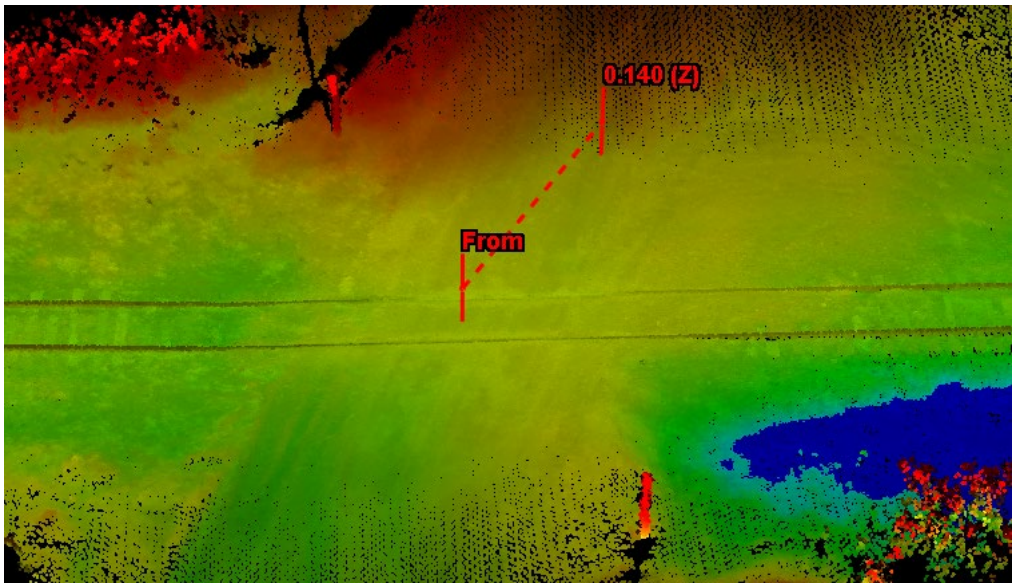

Figure 38: Point cloud view of crossing 304510V showing identified maximum planer deviation

4.1.5 Combined Results

Combining all validation sites from the four categories listed yields a total of 83 crossings that were analyzed to evaluate the accuracy of the algorithm outputs. These crossings were randomly selected from subsets of the data based on characteristics that were known to produce inaccurate results in the original algorithm. The primary goals of this task were improved accuracy at crossings with high planer deviations and sharp roadway intersection angles.

The error statistics listed in Table 7 are based on the results of manual measurements compiled by researchers. The median error is 0.032 meter (1.26 inches). This is less than half of the AASHTO recommended maximum planer deviation, indicating the LiDAR system and associated data processing algorithms are capable of accurately identifying high-profile grade crossings.

Table 7: Error statistics for all validation sites

Criteria	Difference (m)
Min	0.000
25%	0.013
Median	0.032
75%	0.060
Max	0.112
STD	0.030

4.2 Effect on Planer Deviation Measurements

A total of 13,041 grade crossing scans were collected during the initial LiDAR system deployment. These crossings were subsequently reprocessed using the updated algorithms and used to evaluate the effect of the algorithm updates on the reported planer deviation values.

The team calculated the distribution of planer deviation values using the updated algorithm outputs and compared them to the previously reported measurements. The original dataset showed a significant spike in the occurrence of crossings with a reported planer deviation 0.4 – 0.5 meter, accounting for approximately 40 percent of all crossings in the dataset. This spike in the distribution could not be correlated with any naturally occurring characteristics of grade crossings.

The dataset showed only 0.08 percent of the crossings surveyed were within the recommended AASHTO guidelines for planer deviation and 13.2 percent measured more than 1 meter of planer deviation. The manual review of grade crossing scans discussed in Section 2.3 found these erroneous measurements were primarily attributed to sharp roadway intersection angles, vegetated roadways or adjacent areas, or multiple tracks in the crossing.

In comparison, the distribution of planer deviation values (Figure 39) reported by the updated algorithm shows a more typical distribution, without irregular spikes in occurrence of 0.4 – 0.5-meter measurements. Analysis indicates that 4.92 percent of crossings surveyed fall within the recommended AASHTO guidelines. The number of crossings with a planer deviation exceeding 1 meter was reduced to 7.26 percent.

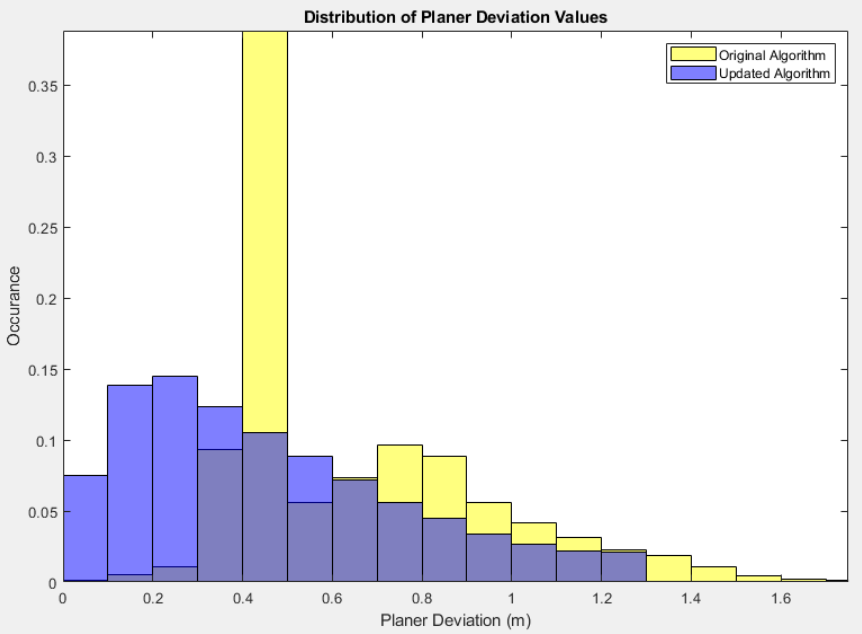

Figure 39: Histogram showing distribution of planer deviation values produced by original algorithm overlaid with updated results

Noting the significant reduction in the number of crossings reported to have very high planer deviation, the team undertook an analysis to determine which grade crossing characteristics had the strongest correlation to reduced planer deviation values.

Researchers segmented the dataset by the change in reported planer deviation then plotted the distribution of various grade crossing parameters to visually identify grade crossing characteristics that were linked to a significant change in planer deviation. The grade crossing parameters that were reviewed included the number of tracks in a crossing and the roadway intersection angle.

A review of the distribution of the number of traffic lanes showed no significant result. The distribution of crossings with a reported change in planer deviation of greater than 1 meter was essentially the same as the overall distribution, indicating that the sites with the greatest change in measurement value were evenly distributed among the number of traffic lanes (Figure 40). Additionally, 16.9 percent of the reprocessed grade crossings do not have information on the number of traffic lanes reported in FRA's Grade Crossing Inventory, reducing the validity of subsequent analysis.

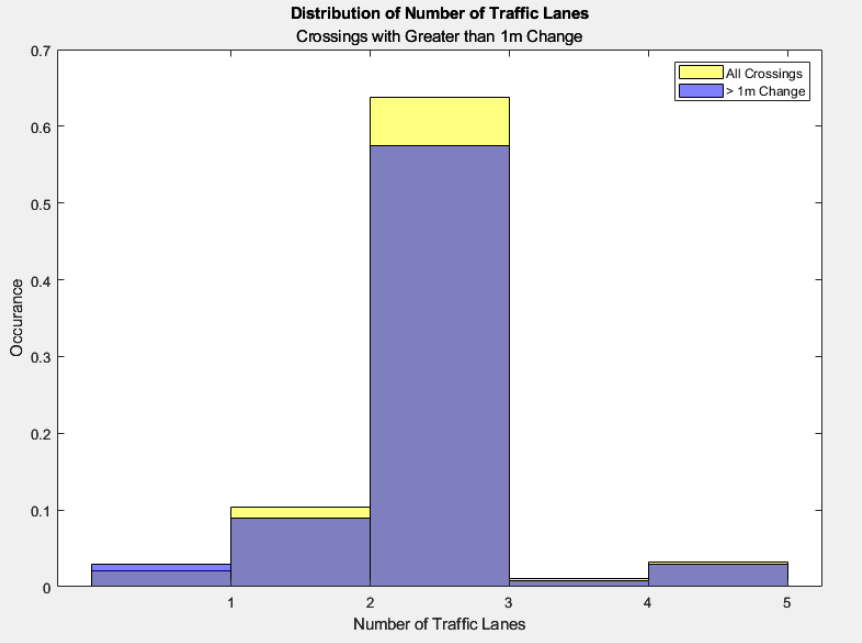

Figure 40: Histogram showing distribution of number of traffic lanes at reprocessed crossings with greater than 1-meter change in planer deviation

Similarly, a review of the number of adjacent rail tracks in the crossing showed only a slight shift in distribution. Figure 41 shows the distribution of adjacent track count for reprocessed crossings with a change in reported planer deviation greater than 1 meter. The distribution shows only a slight increase in the occurrence of single-track crossings with a large change in planer deviation, while the occurrence of multi-main crossings is reduced.

The most significant finding was the distribution of roadway intersection angles at crossings reprocessed with the updated algorithms. The distribution of crossings with greater than 0.25-meter change in planer deviation overlays the distribution of all crossings with very little visible deviation (Figure 42). The occurrence of crossings with a roadway intersection angle of less than 40 degrees accounted for 12.3 percent of the overall dataset. Among reprocessed crossings with a reported change in planer deviation greater than 0.25 meter, the occurrence was 12.1 percent.

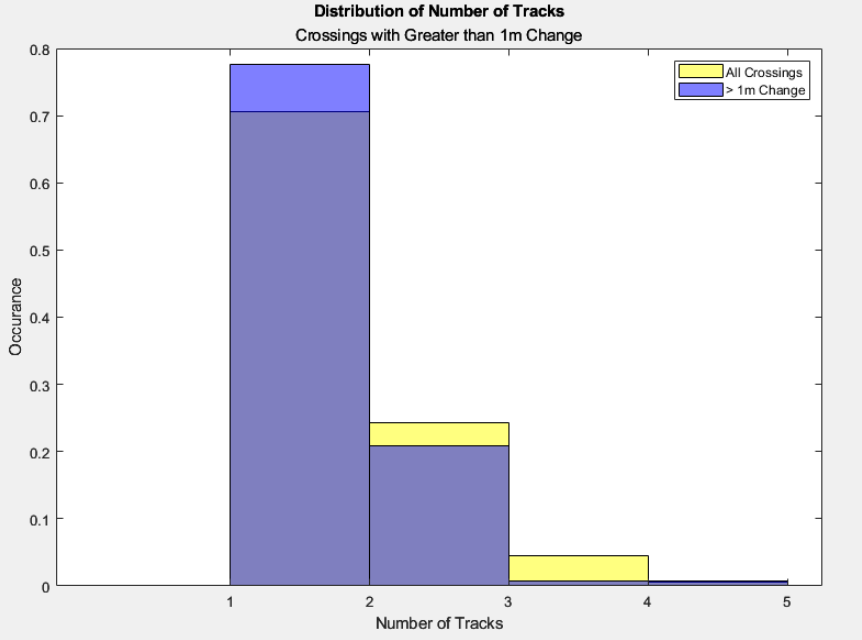

Figure 41: Histogram showing distribution of the number of adjacent rail tracks at reprocessed crossings with greater than 1-meter change in planer deviation

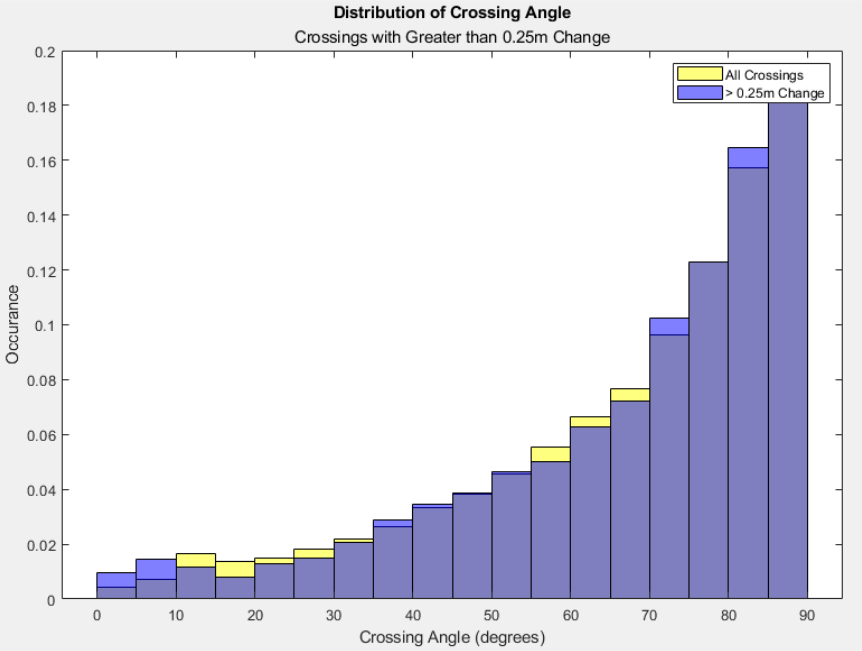

Figure 42: Histogram showing distribution of crossing angle for locations with a change in reported planer deviation greater than 0.25 m

Comparing the distribution of crossings with greater than 0.5-meter change in planer deviation, differences in the distribution begin to emerge. The occurrence of crossings with an intersection angle less than 40 degrees increases from 12.3 percent to 15.0 percent (Figure 43).

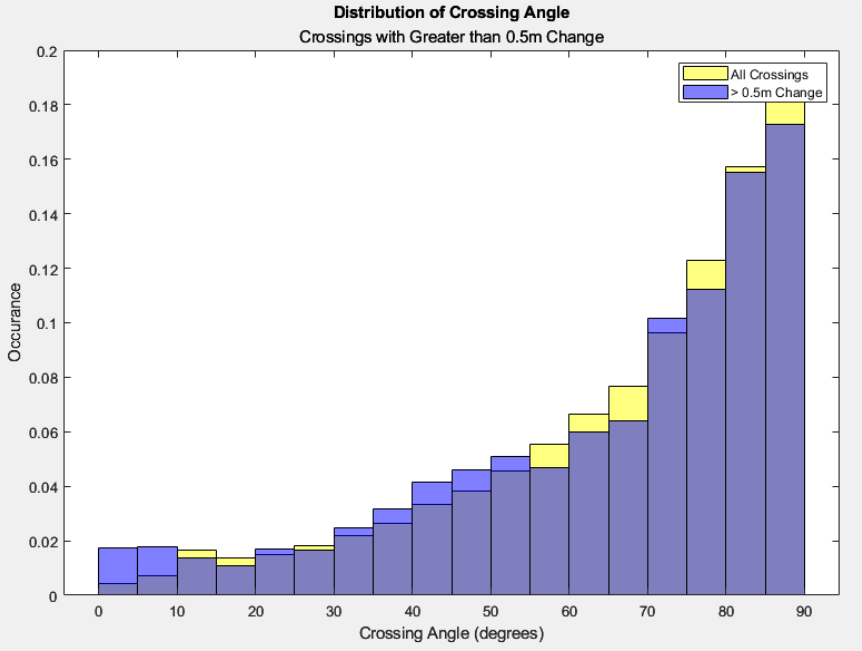

Figure 43: Histogram showing distribution of crossing angle for locations with a change in reported planer deviation greater than 0.5 m

Applying this analysis to reprocessed crossings with a reported change in planer deviation of greater than 0.75 meter, the same data trend becomes more evident. Shown in Figure 44, the portion of crossings with an intersection angle less than 40 degrees increases to 26 percent, more than twice the occurrence rate of the full dataset.

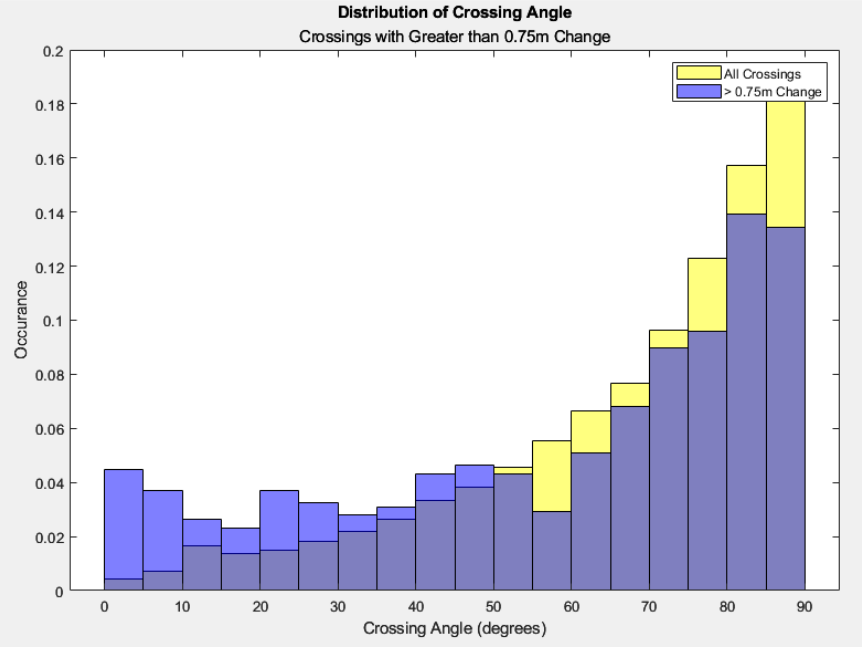

Figure 44: Histogram showing distribution of crossing angle for locations with a change in reported planer deviation greater than 0.75 m

Lastly, an analysis of reprocessed crossings with a reported change in planer deviation of greater than 1 meter was performed. These crossings showed the largest change in reported planer deviation after being reprocessed with the update algorithm, and represent crossing characteristics that were among the worst performing types under the original algorithms. Figure 45 shows the portion of crossings with an intersection angle less than 40 degrees increases to 45.5 percent, nearly 4 time the prevalence in the full dataset. This demonstrates that the most extreme cases, specifically very sharp intersection angles, are overly represented among crossings that had significant calculating errors under the original algorithms.

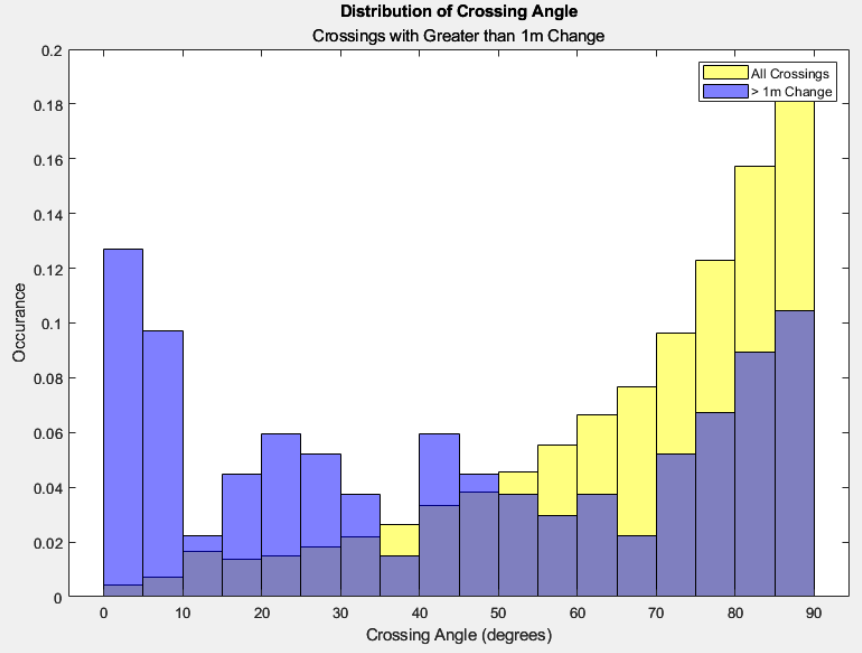

Figure 45: Histogram showing distribution of crossing angle for locations with a change in reported planer deviation greater than 1 m

4.3 Coverage Analysis

The distribution of grade crossing scans collected through this effort are dependent on the typical routing of the ATIP inspection vehicles. The vehicles used for grade crossing inspection were selected based on their distinct uses and routing. DOTX220 is typically routed along Class I mainline tracks and regional railroads that connect the Class I network. Because of this, grade crossings inspected by DOTX220 will skew toward higher track class and heavy haul routes. Conversely, DOTX304 is a smaller hi-rail inspection vehicle and is typically routed over short line railroads, industry tracks, and low-traffic routes. The grade crossings inspected by DOTX304 reflect this difference in routing. Together the two vehicles provide a more comprehensive assessment of grade crossings within the United States' rail network.

An analysis of the distribution of grade crossing inspection throughout the United States was undertaken to better understand whether the current assessment is representative of the rail network. Comparisons were made between the distribution of crossings listed in FRA's Grade Crossing Inventory and those collected through the grade crossing inspection program to quantify differences in distribution.

First, the team analyzed the distribution of crossings by state. Results for the 10 states with the highest number of crossings are presented in Table 8 and Figure 46. The rate of inspection varies from less than 1 percent to more than 7 percent. This is likely a result of the location of mainline routes and ATIP routing priorities.

Table 8: Total number of crossings, number scanned, and percent scanned by state

State	Total Crossings	Crossings Scanned	Percent Scanned
TEXAS	24793	510	2.1%
ILLINOIS	22480	1156	5.1%
OHIO	17115	945	5.5%
CALIFORNIA	15945	668	4.2%
INDIANA	15265	851	5.6%
KANSAS	14667	1067	7.3%
IOWA	14051	951	6.8%
MINNESOTA	13167	591	4.5%
PENNSYLVANIA	12691	433	3.4%
MICHIGAN	12520	88	0.7%

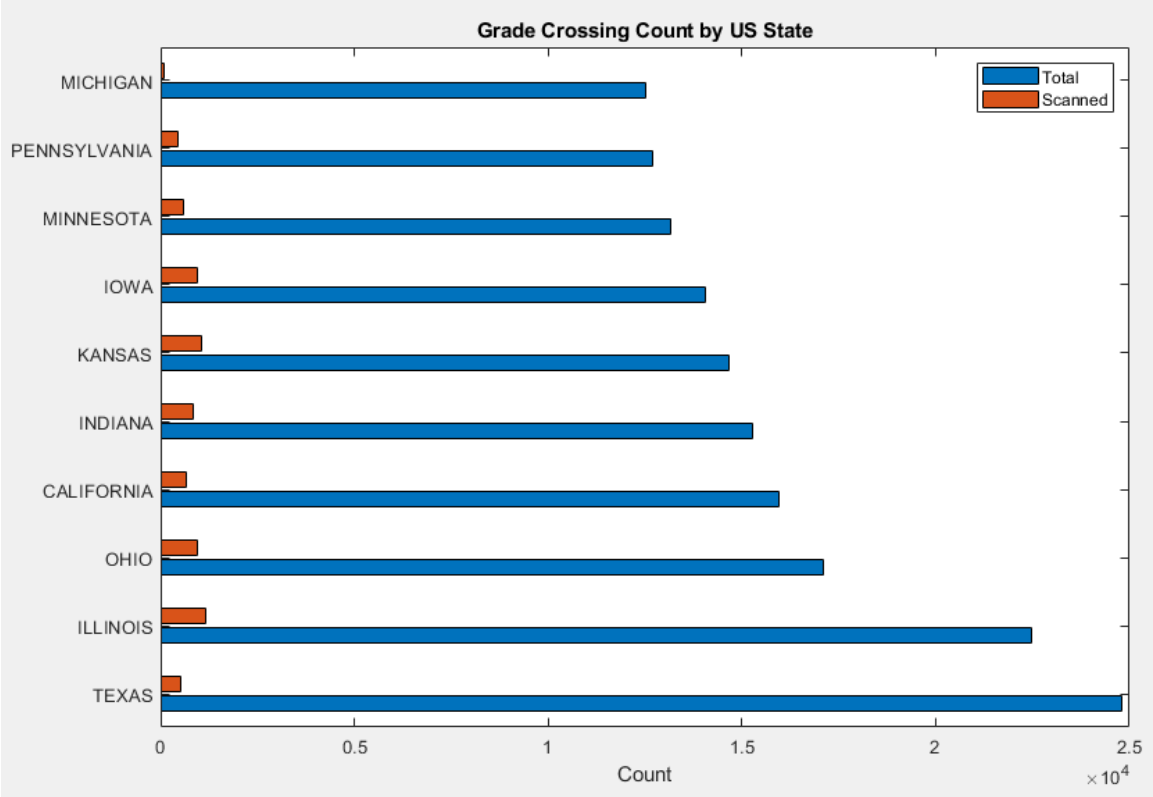

Figure 46: The total number of crossings and the scanned crossing count for the top 10 states

Second, allocation of scanned crossings among the Class I railroads were compared to entries in FRA's Grade Crossing Inventory (Table 9 and Figure 47). UP, BNSF, and CSX all show

approximately 7 percent of their total crossings have been scanned to date, while NS has greater coverage at 12.5 percent.

Table 9: Allocation of total number of crossings and the number of crossings scanned to date among the US Class I railroads

Railroad	Total Crossings	Crossings Scanned	Percent Scanned
UP	60624	4345	7.2%
BNSF	50733	3634	7.2%
CSX	45821	3087	6.7%
NS	39387	4937	12.5%

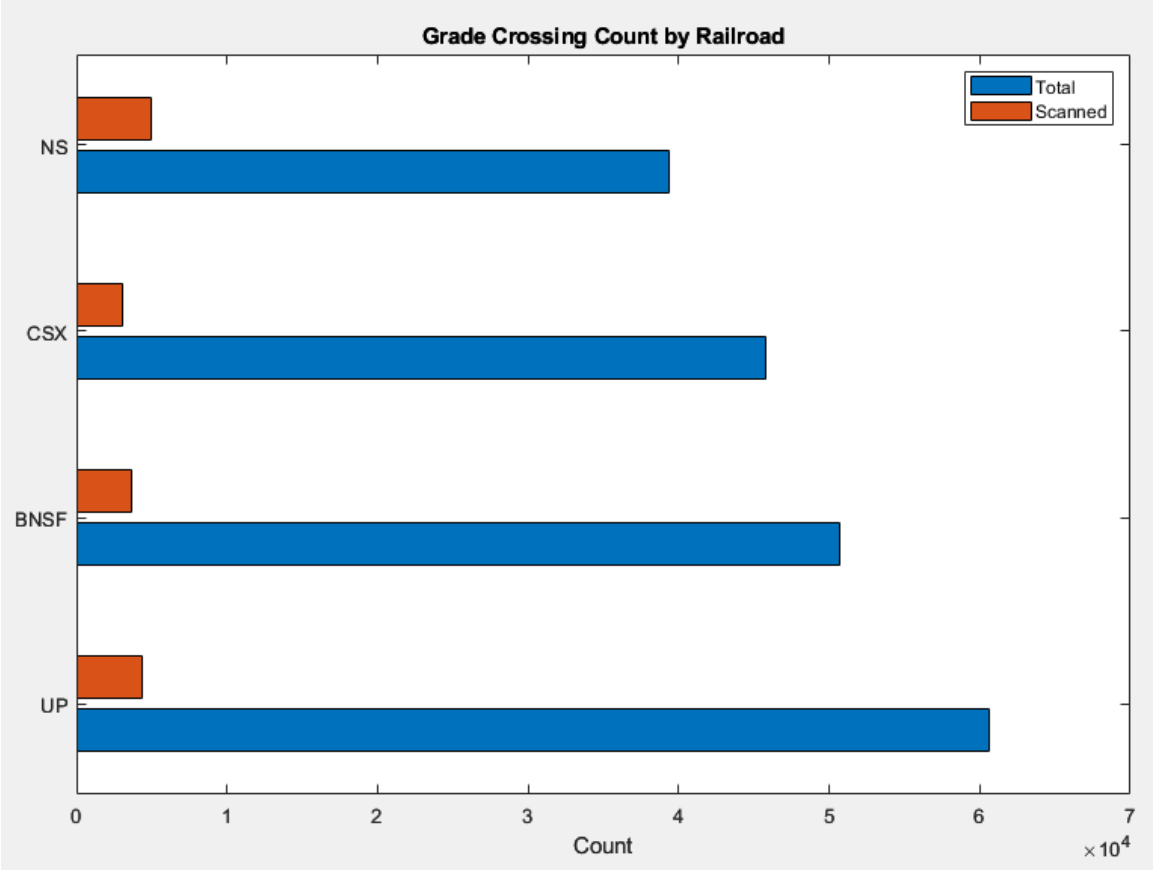

Figure 47: Allocation of total number of crossings owned by US Class I railroads and the number of crossings scanned to date

Finally, to determine the effect of recurring annual ATIP surveys over the same routes, an analysis of the repeat scan rate was performed. Figure 48 shows the total number of scans collected monthly using the two ATIP LiDAR grade crossing systems. Additionally, the breakdown between unique crossings being scanned for the first time, and repeat crossings being surveyed again is shown. This analysis shows that over time the number of crossings scanned each month varies due to the mileage covered by the cars as well as the characteristics of the routes. Urban environments typically have more closely spaced roadways resulting in more

frequent grade crossings. A review of the number of crossings being scanned more than once does show an increase as time progresses. This is an expected result due to the nature of ATIP routing and the use of mainline routes to access other less frequently surveyed subdivisions.

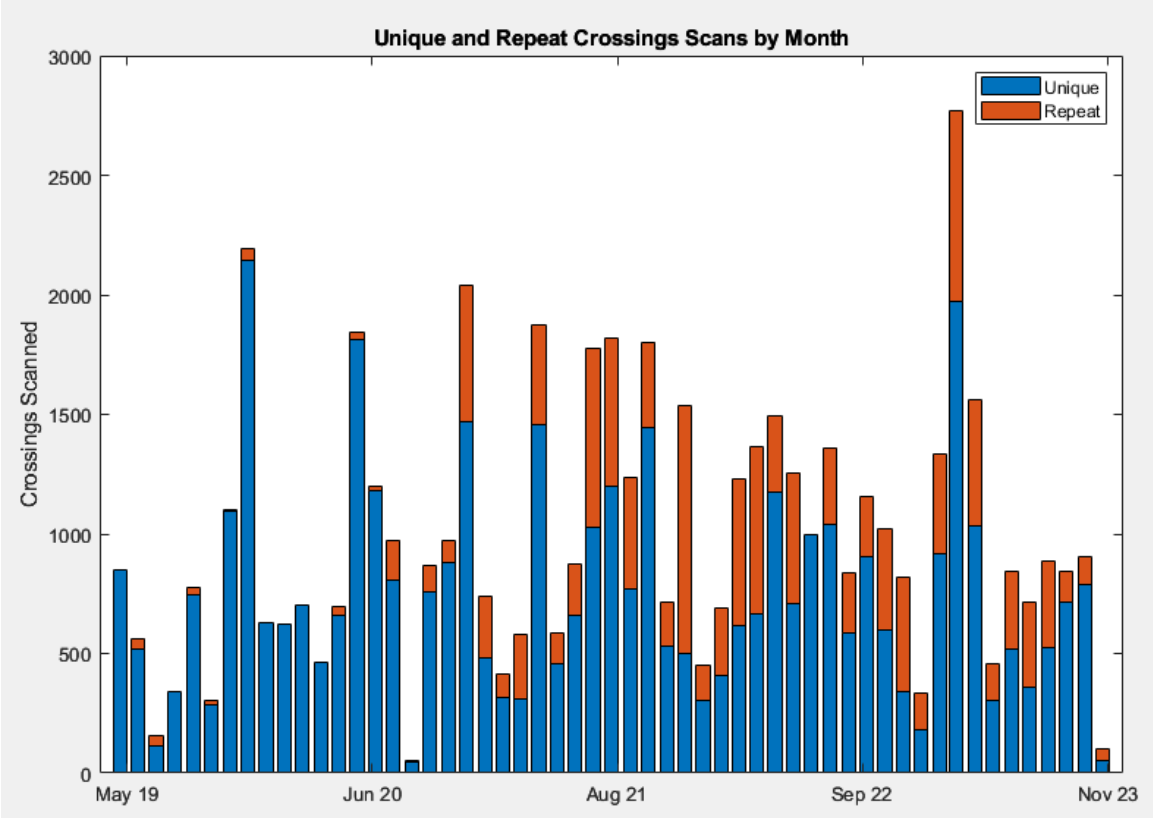

Figure 48: Total number of scans collected monthly including repeat and unique crossings

Comparing the number of repeatedly scanned crossings to the total monthly scan count provides a repeat scan rate, expressed as a percentage. Figure 49 shows this scan rate from May 2019 through November 2023. There is considerable variation in the plot from month to month, with the repeat scan rate varying from 0 percent at the start of the project to a maximum of 68 percent. However, a clear increase can be seen as the survey efforts enter the second year and beyond. ATIP routing does attempt to capture more seldom surveyed routes but often uses mainlines to access those routes, so it is expected that this rate will continue to increase over time but will not approach 100 percent repeat surveys within the foreseeable future. Additionally, it is important to recall that repeat surveys of individual crossings are valuable as they allow for monitoring of the planer deviation over several years, during which time successive track and roadway maintenance activities can alter the crossing's characteristics.

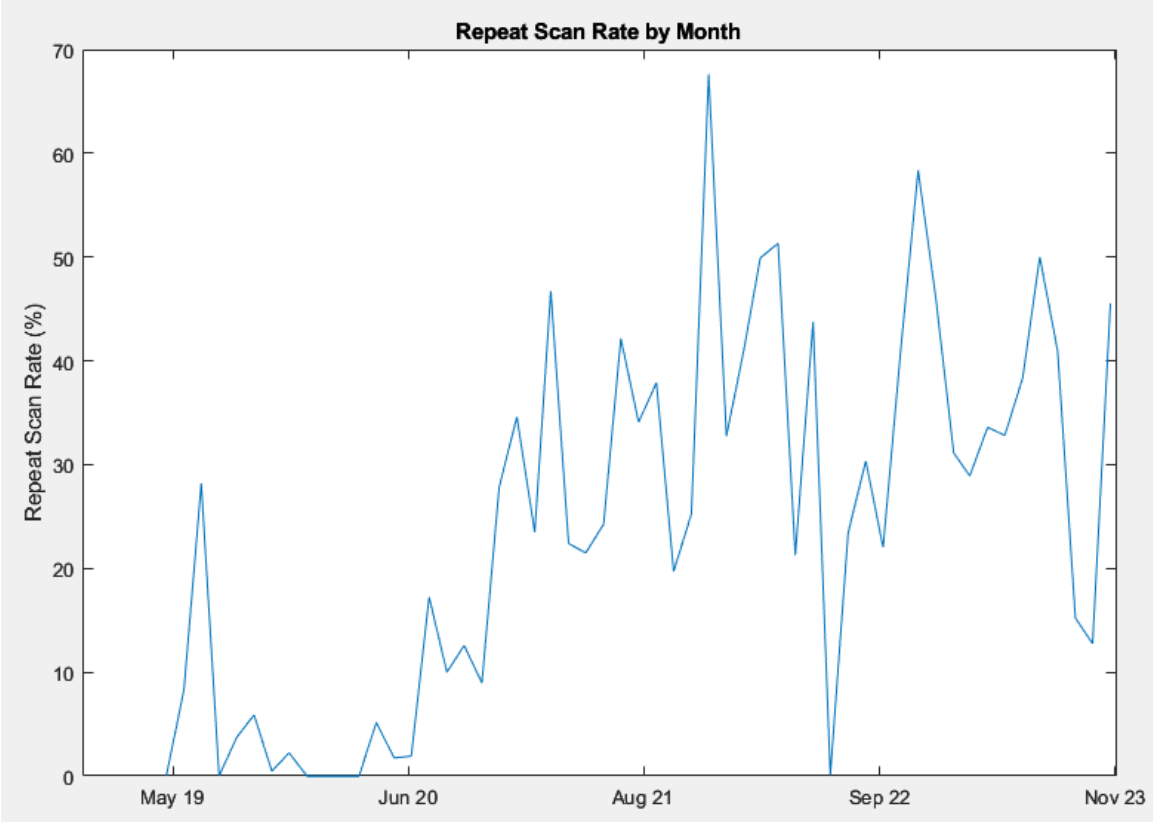

Figure 49: Percentage of crossing scans collected monthly that are repeat surveys

4.4 Evaluation of Drone-Based Photogrammetry

Due to ATIP vehicle routing and survey prioritization based on track usage, a significant portion of the grade crossings in the United States are unlikely to be surveyed by the LiDAR system installed on DOTX220 and DOTX304. Other methods will have to be employed to create a comprehensive nationwide database of grade crossing planer deviation measurements.

4.4.1 Crossing-i Overview

One approach that was evaluated under this task is the Crossing-i system developed by Michigan Technological Research Institute (MTRI). Crossing-i uses a drone-mounted, high-resolution camera and 3D photogrammetry processing to produce point cloud models of grade crossings. Reference markers are placed on the ground surrounding the crossing and their location is surveyed using high-precision GPS. The Crossing-i drone is then flown to various viewpoints around the crossing and photographs of the crossing and ground reference markers are captured (left side of Figure 50). Following data collection, the photographs are stitched together to form a 3D point cloud using the known locations of the ground targets as reference points (right side of Figure 50). This approach can produce models with a ground sample resolution of 2 cm or better. The 3D model can then be analyzed to determine the roadway profile and planer deviation similar to LiDAR point clouds.

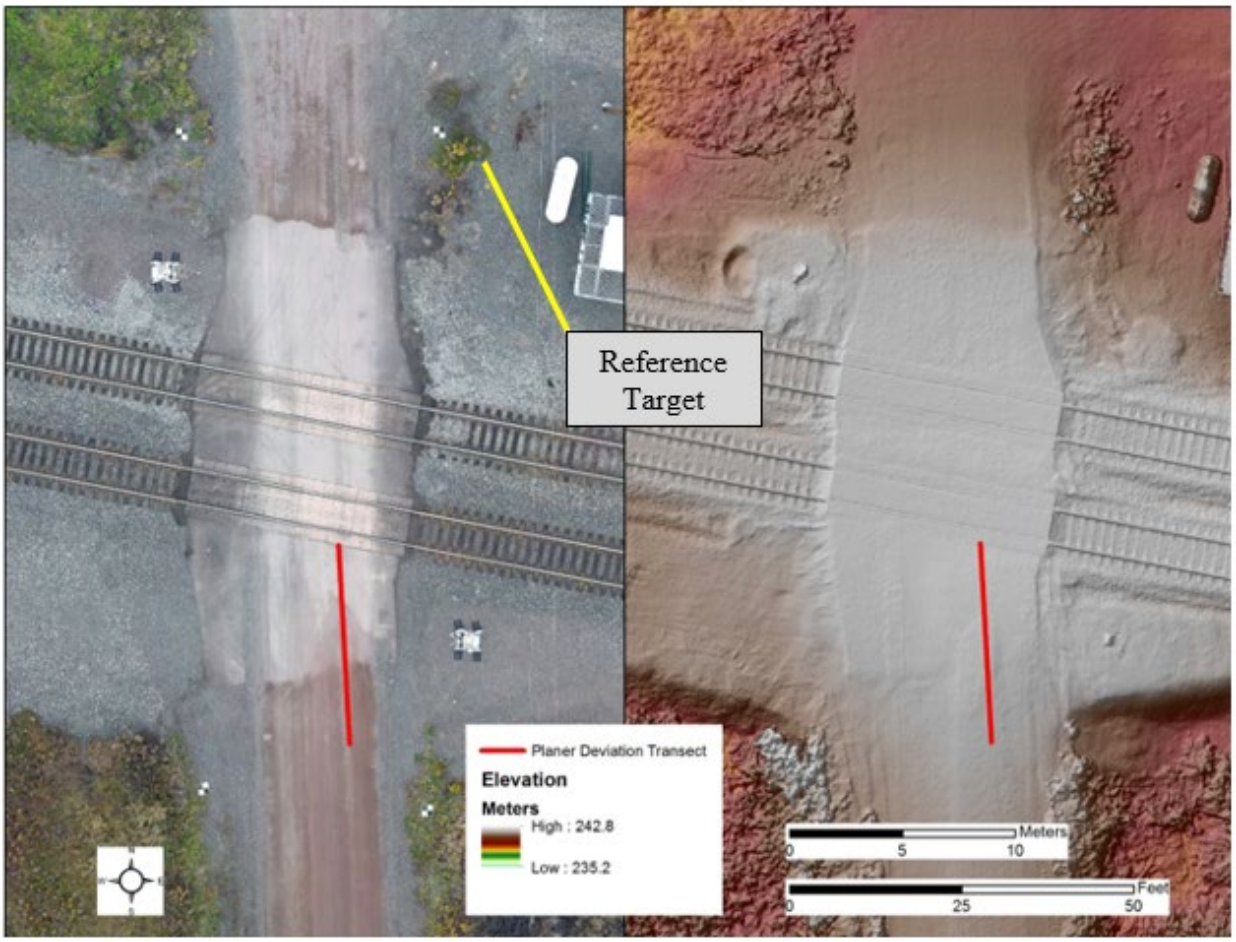

Figure 50: Example of Crossing-i system data showing overhead photo with ground target (left side) and 3D model (right side)

4.4.2 Crossing-i Data Collection

An evaluation of the Crossing-i system was organized by selecting 30 grade crossings that had been surveyed previously by one of the ATIP vehicles (Figure 51). To minimize travel for the Crossing-i support team, the crossings selected were in the vicinity of Ann Arbor, MI, where the team is based. The selected crossings were intended to be representative of the various characteristics that were known to present challenges for planer deviations measurements, specifically, high planer deviation of the roadway, sharp roadway intersection angle, multiple tracks in the crossing, and heavy vegetation near the crossing.

The Crossing-i data collection efforts were conducted in late July and August of 2023. The tracks in the vicinity of Ann Arbor, MI, are all light traffic routes operated by short-line or regional railroads, and are surveyed by ATIP less frequently than most Class I mainline tracks. The most recent LiDAR data available at the selected crossings was collected by the DOTX304 hi-rail vehicle in June of 2021.

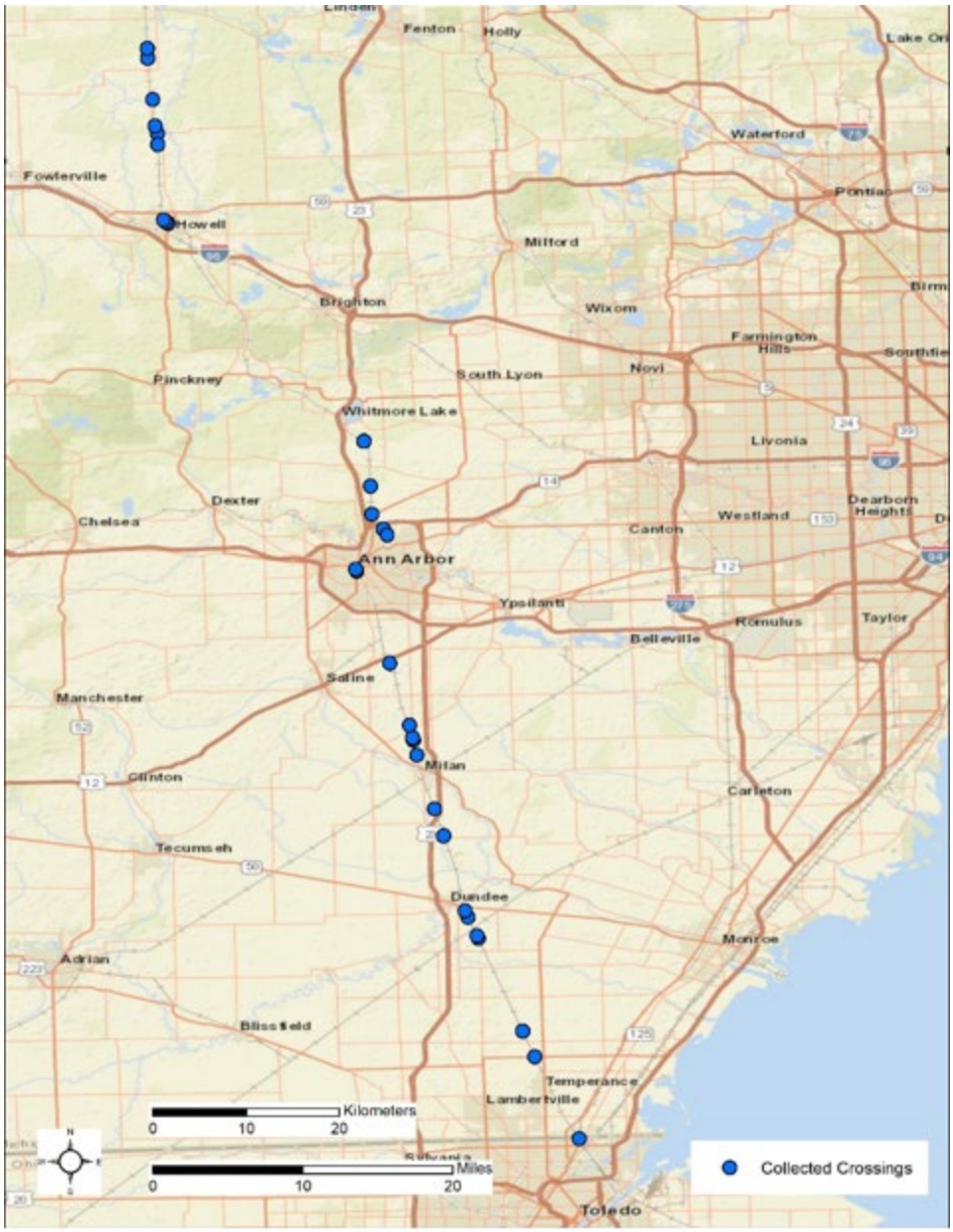

Figure 51: Map showing the grade crossings surveyed by the Crossing-i team

The Crossing-i data collection process involved the team driving to the selected crossing and conducting a visual assessment to identify ideal locations for equipment setup. Next, the ground reference targets were laid down in locations readily visible from various perspectives near the crossing, typically four locations. The ground targets were then surveyed with high-precision GPS. It is crucial to performance of the system that the reference coordinates be established precisely because the subsequent analysis uses those coordinates to link together multiple photographs.

After preparing the site, the team flew the drone to various perspectives around the crossing to capture a comprehensive set of photographs. Following collection of the imagery, the drone was retrieved, the photographs downloaded, and the team proceeded to the next crossing. For the

purposes of this evaluation, the Crossing-i team flew two different drones sequentially, repeating the data collection with cameras of different resolution. The two drones used were a Mavic 2 Pro with a 20-megapixel (MP) camera and a Mavic 2 Enterprise Advantage (M2EA) with a 48 MP camera. This was done to understand the effect of camera resolution on ground sample density of the resultant 3D model. The typical time required at each crossing was 30 – 45 minutes, with a single drone flight requiring 10 – 20 minutes.

During the data collection efforts, no issues were encountered with the drones themselves aside from rain or wind gusts over 30mph during two days of field activities. The team did experience some limitations to accessing crossings for data collection while on location which delayed or prohibited data collection. These issues included a road crew performing maintenance at one location, and a train parked in another crossing. Both issues resulted in a delay of approximately 30 minutes.

Following data collection activities in the field, the photographs and ground target location data were post-processed using a software package developed by the Crossing-i team. Due to the two drones having different resolution cameras, data processing for the Mavic 2 Pro photographs took approximately 2.5 hours, while the Mavic 2 Enterprise Advantage required approximately 4 hours.

Two sets of point clouds were produced. The first set was at the full point cloud density and the second was down sampled. The point cloud density for the initial delivery of the Mavic 2 Pro was on average 35,477 points per square meter (ppm^2) and the M2EA was 9,600 ppm^2. The delivered full resolution point cloud files were on average 1.5 GB in size. A second set of files was down sampled to produce point cloud files comparable in size to the LiDAR system. Down sampling was achieved by reducing the point cloud density of the Mavic 2 Pro to 102 ppm^2 and 105 ppm^2 for the M2EA. The point clouds were also cropped closer to the crossing. The remaining point cloud extents were at least 30 feet from the outside rail along the roadway and 50 feet along the tracks on either side of the crossing. Additionally, point color information was removed from the point clouds to further reduce file size. These modifications combined reduced the point cloud file size to an average of 1.5 MB.

4.4.3 Comparison to LiDAR Measurements

For all crossing being evaluated, the planer deviation measurements were calculated from the LiDAR point clouds using the updated algorithms used on the ATIP vehicles. For the Crossing-i data, planer deviation measurements were taken manually using a point cloud viewer as well as using a software tool developed by the Crossing-i team. The software first identifies the location of the rails, roadway, and geometry of the crossing from a digital elevation model (DEM) input. Assessment of the crossing is then performed to calculate planer deviation of the roadway. All planer deviation measurements for the evaluated crossings are listed in Table 10.

Comparing results obtained from the Mavic 2 Pro and the M2EA drones to the ATIP LiDAR system, the team found variation in how well the systems agree. The M2EA was generally closer to the ATIP LiDAR system results, with an average difference in planer deviation of 0.072 meter (0.236 feet). The Mavic 2 Pro results showed a larger average difference of 0.154 meter (0.505 feet) when compared to the ATIP LiDAR system measurements.

These differences in the planer deviation values between the M2EA and the Mavic 2 Pro drones are mostly likely due to differences in how the imagery was collected and processed. The Mavic

2 Pro was flown at a lower altitude and covered a smaller area centered on the crossing. In comparison, the M2EA was flown higher and covered a wider area, allowing for a greater number of ground reference targets to be used. This allowed for better correction of errors in geometry and scaling of the point cloud.

Table 10: Planer deviation values for all crossings surveyed under the Crossing-i evaluation

Crossing_ID	Street	ATIP LiDAR (m)	M2EA Manual (m)	Mavic2 Manual (m)	MTRI Tool (m)
000114M	State Line Rd.	0.588	0.540	0.900	0.366
000126G	Samaria Rd.	0.210	0.270	0.280	0.161
000129C	Jackman Rd.	0.200	0.220	0.210	0.433
000148G	Gloff Rd.	0.163	0.160	0.120	0.282
000149N	Dunbar Rd.	0.164	0.350	0.250	0.201
000151P	Dixon Rd.	0.085	0.080	0.230	0.271
000152W	Roosevelt Rd.	0.450	0.530	1.130	0.303
000165X	Dundee Azalia Rd.	0.360	0.410	0.360	2.289
000170U	Crowe Rd.	0.061	0.060	0.030	0.259
000177S	Arkona St.	0.247	0.130	0.180	0.430
000181G	Willow Rd.	0.113	0.200		
000182N	Platt Rd.	0.020	0.050		
000184C	Begole Rd.	0.387	0.370	0.370	0.284
000190F	Warner Rd.	0.299	0.140	0.390	0.233
000218U	W. Jefferson Ave.	0.113	0.110	0.330	0.387
000219B	Ashley St.	0.036	0.090	0.220	0.387
000220V	William St.	0.359	0.430	0.840	0.745
000239M	Traver Rd.	0.330	0.550	0.930	0.393
000240G	Dhu Varren Rd.	0.145	0.150	0.170	0.244
000243C	Warren Rd.	0.164	0.120	0.130	0.129
000245R	Northfield Church	0.790	0.810	0.820	0.316
000250M	6 Mile Rd.	0.088	0.040	0.040	0.054
000286V	West St.	0.172	0.190	0.270	0.124
000287C	Alger St.	0.259	0.340	0.340	0.486
000288J	Riddle St.	0.096	0.210	0.210	0.238
000295U	Allen Rd.	0.330	0.330	0.330	0.132
000296B	Oak Grove Rd.	0.174	0.040	0.080	0.310
000297H	Sanford Rd.	0.226	0.400	0.520	0.248
000308T	Richards Rd.	0.350	0.310	0.340	0.144
000310U	Lovejoy Rd.	0.511	0.780	0.950	0.543

At four crossings (000152W, 000220V, 000239M, and 000114M) the difference in planer deviation values between the M2EA and Mavic 2 varied between 0.36 m (1.18 ft) to 0.60 m (1.97 ft). Generally, the M2EA produced results closer to the ATIP LiDAR system at 15 of the crossings while the Mavic 2 produced closer results at 8 crossings.

While analyzing data collected using the M2EA, the 000310U - Lovejoy Road crossing stood out with a maximum difference of 0.269 meter (0.883 feet) when compared to the LiDAR

measurements. This is a crossing of an unpaved road where only 2.74 meters (9 feet) on either side of the outside rails are paved. The remaining 3.35 meters (11 feet) of the road within the analysis area is unpaved and has a very rough surface texture surface compared to concrete or asphalt. Figure 52 shows hill shade representations of point cloud data derived from the M2EA drone (left) and the ATIP LiDAR system (right). These datasets were collected two years apart and the unpaved road surface has been graded at least once over that time. There are deep ruts on the southern side of Lovejoy Road visible in LiDAR point cloud data which may have impacted the planer deviation measurement. A review of the M2EA point cloud shows the road surface has been graded to remove the rutting and other distress. This difference highlights the effect of roadway maintenance activities on planer deviation values as discussed in Section 2.1.

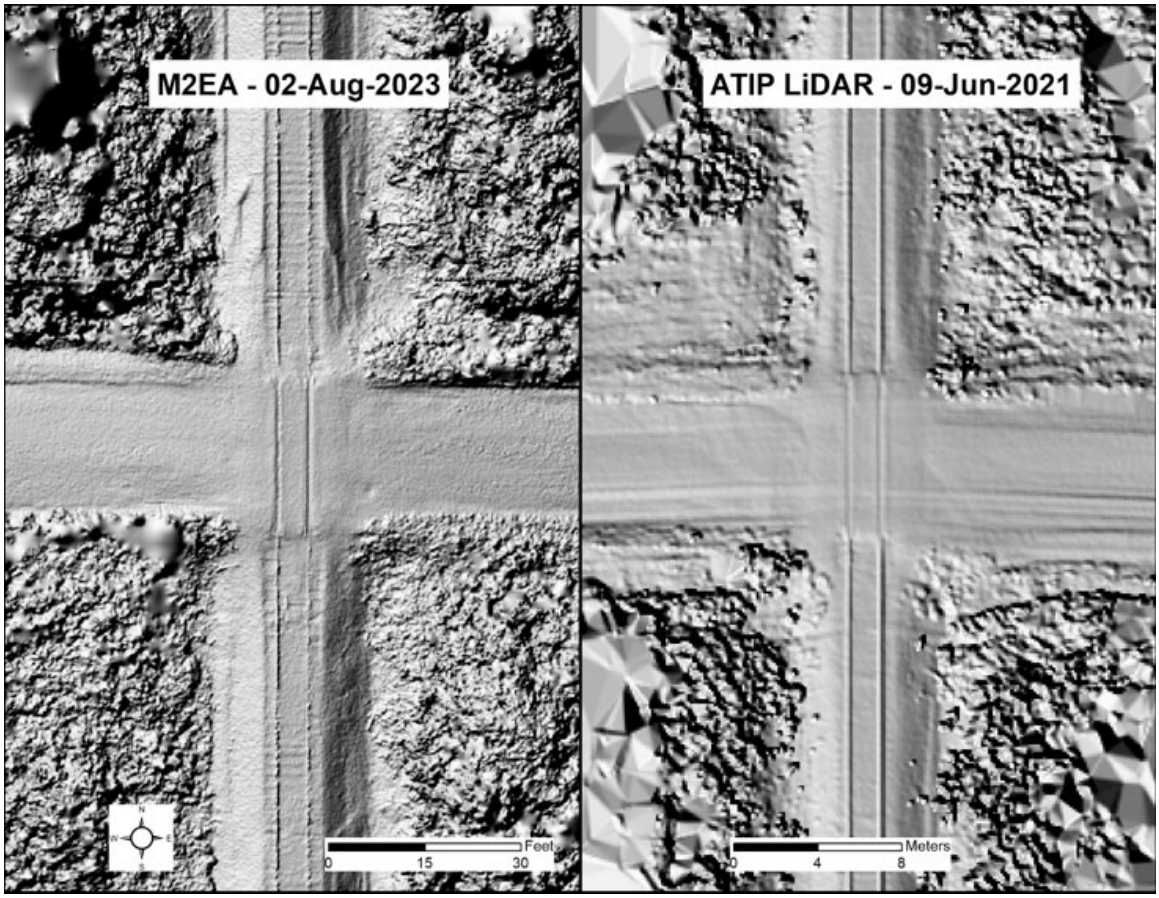

Figure 52: Hill shade representations of the point cloud data collected at crossing 000310U (Lovejoy Road)

The next largest difference in planer deviation values between the M2EA and the ATIP LiDAR occurred at crossing 000239M - Traver Road. This is also a crossing of an unpaved road and there is a 0.22 meter (0.72 feet) difference in planer deviation between the two systems. The hill shade representation of both systems' point cloud data is shown in Figure 53.

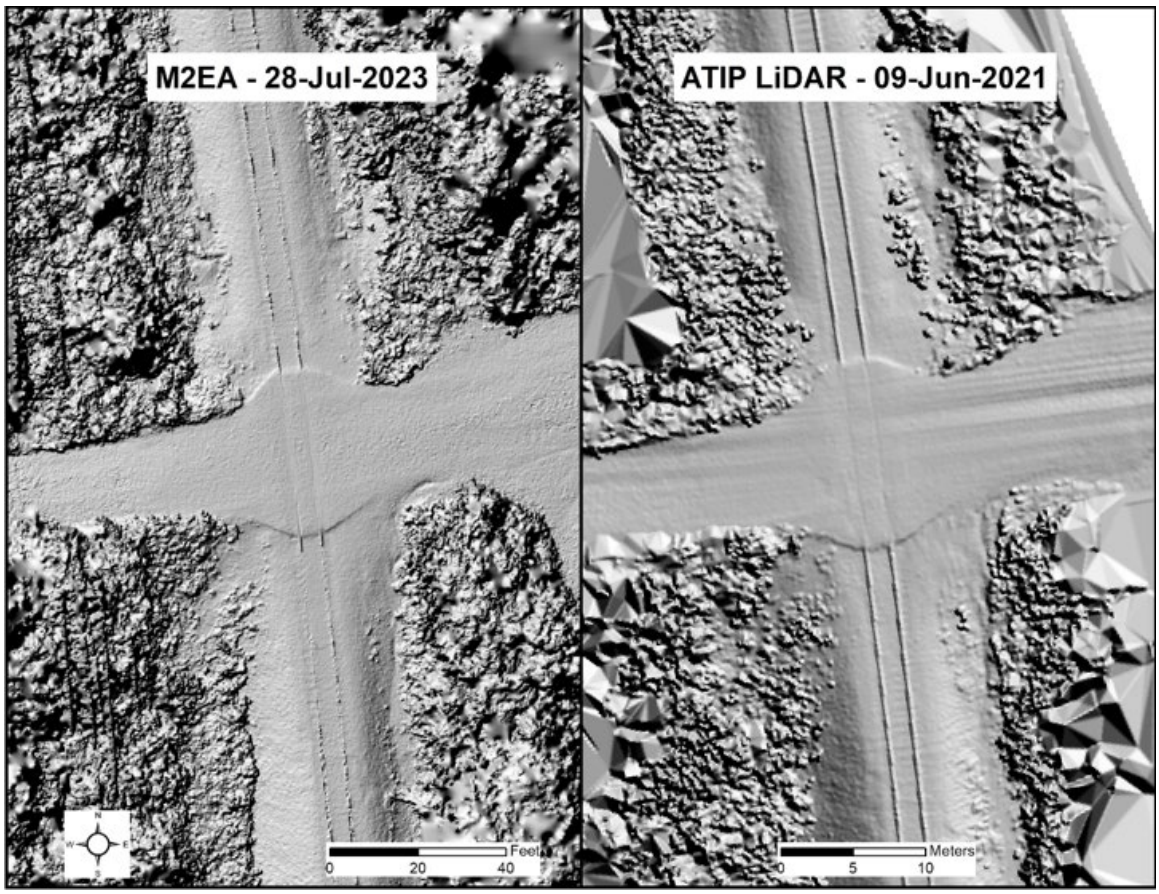

Figure 53: Hill shade representation of point cloud data collected at crossing 000239M (Traver Road)

A review of the roadway surface in the point clouds of both systems shows more severe rutting consistent with the location of vehicle traffic in the LiDAR data, while the M2EA point cloud shows a more evenly crowned road. This discrepancy is likely a result of road maintenance activities occurring within the two year timespan between the two data collection events. The location identified by the LiDAR system as having the largest planer deviation on either side of the crossing is shown in Figure 54. Both locations are within the unpaved roadway, with the location in the bottom of the figure has the greater planer deviation.

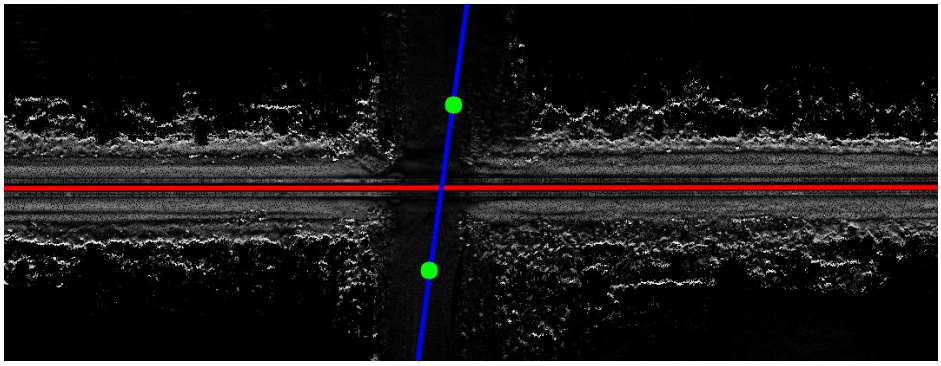

Figure 54: Bird's-Eye-View of crossing 000149N - Dunbar Road showing the roadway fit and identified maximum planer deviation on both sides of the crossing

The MTRI planer deviation analysis was performed on all point clouds collected using the Mavic 2 drone. Additionally, manual measurements were taken using a point cloud viewer and the results from each approach were compared. Table 11 shows the difference between the planer deviation measurement obtained using both approaches. The average difference in planer deviation value is 0.274 meter (0.899 feet), while most automated measurements produced by the MTRI tool showing at least 0.10 meter (0.328 feet). This finding is a function of how the bounding box for the automated analysis is generated. After the crossing location is identified and the crossing geometry is determined by the algorithm, a bounding box is generated over the area of interest in the road. In its current version the bounding box may not be generated correctly in cases of complex crossings with multiple roadways intersections or curved roadway approaches.

Table 11: Comparison of automated Crossing-i planer deviation measurements vs. manual measurement

Crossing_ID	Street	Mavic2 (m)	MTRI Tool Pro	Manual-MTRI Tool (m)
000114M	State Line Rd.	0.900	0.366	0.534
000126G	Samaria Rd.	0.280	0.161	0.119
000129C	Jackman Rd.	0.210	0.433	0.223
000148G	Gloff Rd.	0.120	0.282	0.162
000149N	Dunbar Rd.	0.250	0.201	0.049
000151P	Dixon Rd.	0.230	0.271	0.041
000152W	Roosevelt Rd.	1.130	0.303	0.827
000165X	Dundee Azalia Rd.	0.360	2.289	1.929
000170U	Crowe Rd.	0.030	0.259	0.229
000177S	Arkona St.	0.180	0.430	0.250
000184C	Begole Rd.	0.370	0.284	0.086
000190F	Warner Rd.	0.390	0.233	0.157
000218U	W. Jefferson Ave.	0.330	0.387	0.057
000219B	Ashley St.	0.220	0.387	0.167
000220V	William St.	0.840	0.745	0.095
000239M	Traver Rd.	0.930	0.393	0.537
000240G	Dhu Varren Rd.	0.170	0.244	0.074
000243C	Warren Rd.	0.130	0.129	0.001
000245R	Northfield Church	0.820	0.316	0.504
000250M	6 Mile Rd.	0.040	0.054	0.014
000286V	West St.	0.270	0.124	0.146
000287C	Alger St.	0.340	0.486	0.146
000288J	Riddle St.	0.210	0.238	0.028
000295U	Allen Rd.	0.330	0.132	0.198
000296B	Oak Grove Rd.	0.080	0.310	0.230
000297H	Sanford Rd.	0.520	0.248	0.272
000308T	Richards Rd.	0.340	0.144	0.196
000310U	Lovejoy Rd.	0.950	0.543	0.407

The largest difference occurred at crossing 000165X - Dundee Azalia Road. At this location, the two measurement approaches showed a discrepancy of 1.929 meters (6.329 feet). This is the result of an incorrect bounding box placed by the MTRI algorithm. Figure 55 shows that the roadway intersection angle is very sharp and the roadway curves immediately before and after the crossing. The current version of the tool creates a box extending 30 feet from the outside rail and does not adjust for a curved road within that distance. For this crossing, the bounding box extends out beyond the roadway surface, resulting in a planer deviation measurement taken outside of the roadway surface.

Figure 55: Overhead view of crossing 000165X - Dundee Azalia Road collected using the Crossing-i system

During the evaluation of the Crossing-i system, the M2EA drone was shown to produce planer deviation measurements that are consistent with the ATIP LiDAR. Most of the crossings which

had greater differences in values were unpaved roads where the condition of the road surface has the potential to change rapidly compared to paved surfaces. Over the two-year period between the ATIP LiDAR and Crossing-i data collection events, the road surfaces changed. These changes included both degradation in the form of rutting and wash boarding, as well as maintenance activities such as grading. Maintenance activities are expected to affect the planer deviation measurements and underscore the importance of resurveying the road approaches after completion of maintenance activities to identify changes in planer deviation.

5 Conclusion

Collisions between motor vehicles and trains are a leading cause of injuries in the railroad industry. A major cause of grade crossing incidents are vehicle hangups due to high-profile, or "humped", grade crossings. HPGCs should have appropriate signage installed to warn motorists of the risk of becoming stranded in the crossing. However, many HPGCs are not adequately identified in FRA's Grade Crossing Inventory and lack appropriate warning signs. Additionally, successive track maintenance activities, such as the addition of ballast during tamper, as well as layering of asphalt during roadway maintenance, can alter the profile of the crossing and increase the risk of a vehicle hangup. Best practice is to resurvey the roadway vertical profile, or planer deviation, after track or road maintenance activities are concluded. However, this is not always possible due to lack of coordination between railroads and state or local highway departments. Also, often in rural areas the availability and cost of a survey crew does not allow for this important safety check. Therefore, FRA has worked to improve the ability to identify HPGCs and increase awareness of sites that pose a risk to motorists.

To support this effort, LiDAR 3D scanner arrays were installed onboard two rail survey vehicles operated under ATIP. These vehicles conduct year-round enforcement survey activities inspecting track geometry nationwide to ensure safe operating conditions for rail traffic. Installation of the autonomous LiDAR scanner system aboard these vehicles has provided a platform to collect and analyze the vertical profile of the roadways at grade crossings. Following initial deployment and data collection efforts beginning in May 2019, an analysis of the grade crossing planer deviation measurements was performed to evaluate system performance. This analysis indicated that the original data processing algorithms struggled to provide accurate measurement of the grade crossing planer deviation under certain conditions, specifically, grade crossings with sharp roadway intersection angles or locations with heavy vegetation in or near the roadway.

To improve the accuracy of measurements collected under these conditions, researchers worked to better understand the limitations of the existing algorithms and develop a plan to implement improved methods. The current efforts focused on improving the algorithms, validating the accuracy of the data outputs under challenging conditions, and reprocessing all grade crossing data collected since May 2019. The LiDAR systems have collected 70,152 3D point clouds scans to date. Among these are 51,385 unique crossings, with the remainder being repeated scans at previously surveyed crossings.

LiDAR point cloud processing has become a critical aspect of many industries including land surveying, agriculture and forestry, and watershed mapping and analysis. Recent developments in point cloud processing were leveraged in the updated algorithms. Specifically, a PMF was used to remove vegetation, roadway and crossing signage, vehicles, and other objects not associated with the roadway surface. Next, a SVM algorithm was used to identify the planer roadway surface and apply a best fit to divide the roadway. Following identification of the roadway and approximation of the intersection angle, the correct offset distance from the track was calculated and planer deviation measurements taken.

Following development of the updated algorithms, the original dataset collected between May 2019 and September 2020 was reprocessed. The team conducted a detailed analysis of the reported planer deviation measurements produced by both algorithms. The findings revealed that

the sites associated with the largest change in planer deviation were also those with the sharpest roadway intersection angle. This was an expected result based on a preliminary survey indicating the original algorithms struggled at crossings with sharp angles between the roadway and track.

The validation efforts were subsequently expanded to a wider validation dataset including all crossing scans collected since September 2020 but not processed with the original algorithms. A sample set of 85 grade crossings was constructed by subdividing the set of all crossings into categories based on crossing configuration. Crossings were randomly selected from within each category while taking care to represent the characteristics which had historically produced inaccurate results. This sample set of crossings was reviewed and planer deviation measurements taken manually. The results demonstrate that the updated algorithms produce planer deviation measurements accurate to within 32 mm (1.26 inch) of the true measurement based on the median error.

Following algorithm updates and a detailed analysis to validate the accuracy of the measurements produced, researchers studied the distribution of grade crossing inspection produced by the ATIP LiDAR system within the United States railroad network. Findings show that inspection of grade crossings owned by the US Class I railroads varies between 6.7 - 12.5 percent. Furthermore, due to the tendency for ATIP vehicles to survey some of the same mainline routes annually while moving between less surveyed subdivisions, the rate of unique crossings collected monthly has decreased to approximately 35 percent.

Considering the inspection coverage of grade crossings in the United States and the decreasing rate of unique crossings being surveyed, other methods of inspection that could provide measurements of planer deviation at crossings unlikely to be surveyed by the ATIP vehicles have to be considered. One potential technology is the Crossing-i system developed by MTRI. Crossing-i is a drone-based photogrammetry method that can create 3D point clouds of grade crossings using aerial photography.

Researchers partnered with MTRI to evaluate the Crossing-i system by surveying a selection of 30 grade crossings that had previously been inspected by one of the ATIP LiDAR systems. The team conducted data collection using the Crossing-i system and compared the data with the ATIP LiDAR measurements. Researchers found that the Crossing-i system can survey crossings unlikely to be surveyed by ATIP vehicles due to location, route traffic, or other factors. Additionally, the Crossing-i system's point clouds produce planer deviation measurements with an average difference of 0.072 meter (2.83 inches) when compared to the ATIP LiDAR system. However, some crossings with complex, curved-approach roadways were challenging for the MTRI analysis tools, and modification would be required to automatically report planer deviation measurements at these crossings.

Both the ATIP LiDAR system and Crossing-i platform can be used to inspect grade crossings and measure the planer deviation of the roadway. The ATIP LiDAR system is very efficient and cost effective because measurements are collected autonomously during already scheduled rail network enforcement activities. The Crossing-i system is a complementary approach that can provide assessments of low traffic routes that are unlikely to be surveyed by ATIP vehicles.

The use of two complementary inspection methods provides FRA a more robust and flexible means of achieving its goal to improve detection of humped crossings and reduce potential risk to motorists. Ongoing survey operations conducted under the ATIP program will continue to provide most of the coverage at grade crossings in the United States. This includes both unique

measurement of previously unidentified high-profile grade crossings as well as repeat assessment of crossings that may become humped due to track or roadway maintenance. Other inspection methods such as the Crossing-i drone-based system can be used to fill gaps in the assessment of grade crossings due to limitations resulting from ATIP coverage and routing.

Appendix A.
Stakeholder Outreach Survey

LiDAR Grade Crossing Inspection

Stakeholder Outreach

Background

FRA has previously installed a LiDAR laser scanner system on two of the Automated Track Inspection Program (ATIP) survey vehicles to collect 3-D point cloud data in grade crossings. The data collected is used to determine the grade of the roadway and identify high-profile grade crossings (HPGC). Crossings that are identified as HPGC can be further investigated to determine if appropriate signage is present to warn motorists of the risk of a vehicle hang-up.

Objective

FRA is in the process of automating the transfer of point cloud data from the ATIP survey vehicles and developing a long-term data storage solution. The goal of this effort is to make grade crossing point cloud data available to railroad stakeholders and industry researchers more quickly than is currently possible. To ensure the solution being developed will meet the needs of all consumers of the data, FRA is requesting feedback from industry stakeholders prior to developing a solution. The primary areas of concern are the data file format, the physical extents of scan data surrounding the crossing, and the associated crossing metadata being stored.

File Format

FRA proposes to use an open-source data format to store point cloud data. This will allow industry professionals and researchers to utilize the data without purchasing proprietary software.

The proposed format is a .LAZ file. This file format is readily viewed using various free software packages. Additionally, it is a compressed file format, reducing the volume of data stored and expediting transfer times without any loss in resolution.

Grade Crossing Point Cloud Extents

As each grade crossing is surveyed additional segments of track are captured on either side of the crossing. During post-processing, the grade crossing location is identified and the point cloud is cropped to a length along the track of approximately 130m including the crossing. The extent of point cloud data adjacent to the track is determined by the visibility and range of the LiDAR scanners and is not cropped during post-processing.

Metadata

For each grade crossing that has been surveyed, FRA intends to extract the following parameters from the Grade Crossing Database:

- Crossing ID
- Railroad Owner
- Division

- Subdivision
- Milepost
- Crossing Angle Range (in 30 degree increments)
- Street
- City
- State
- Number of gates
- Number of roadway lanes
- Presence of High-Profile Crossing signage

Additionally, the following parameters will be extracted from the point cloud data and stored along with the metadata above:

- Vertical Profile (maximum planer deviation in meters)
- Latitude
- Longitude
- Elevation

Data Collected

Below is an example point cloud collected using the LiDAR measurement system. Visible in the point cloud data are crossing gates, roadway, right of way, as well as signal cabinets, warning signs, and trackside vegetation. The example point cloud shown below is characteristic of data collected by the system on-board the ATIP survey vehicles. After loading the data into a 3-D viewer, measurements can be taken to determine the roadway grade, crossing angle, sight line distances and track clearances.

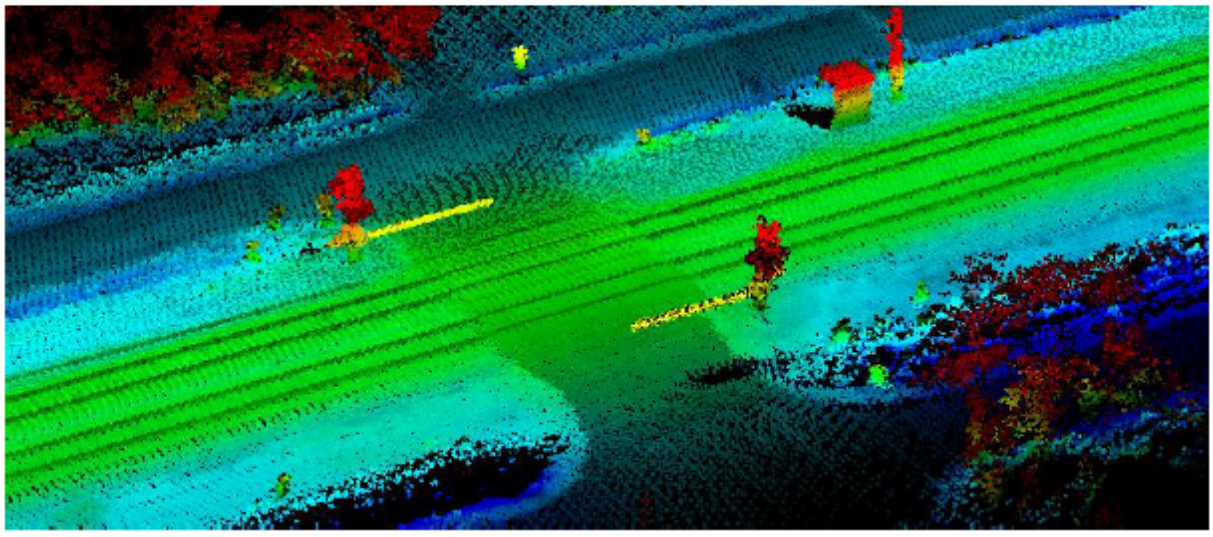

Appendix B.
Stakeholder Survey Recipients

AREMA Committee 2 – Track Measurement and Assessment Systems

- Lariza Stewart

AREMA Committee 36 – Highway-Rail Grade Crossing Warning Systems

- Shawn Hall (BNSF)
- Dale Hill (Alfred Benesch & Company)
- David Flores (Keolis Commuter Services)

TRB Rail Group

- Pasi Lautala (Michigan Tech)

FRA Contacts and Academic Partners

- James Dahlem
- James Payne
- Brian Gilleran
- Ruby Li
- Andrew Martin

Academic Partners

- Chris Barkan
- Ray Benekohal
- Xiang Liu
- Yu Qian
- Joshua Li

Appendix C.
Crossing-i System Evaluation Report

Drone Based Grade Crossing Inspection – Final Report

Richard Dobson (PI), Dr. Colin Brooks, Dr. Pasi Lautala, Nicholas Dobson, and Chris Cook

Michigan Tech Research Institute (MTRI)

Submitted: November 17, 2023

Introduction

Identifying rail grade crossings with steep profiles is critical as they can create the potential for hang-up conditions for vehicles. The MTRI team developed the drone-based Crossing-i system to identify crossings with potential hang-up conditions and identify vehicles of certain wheel bases and heights could become stuck on the roadway at crossings. Through previous projects, this system had been deployed to over 50 crossings across the five states in the Midwest previously.

Another method to identifying potentially hazardous crossings is planer deviation. An ideal rail grade crossing has a slope of 0.89% between 0.6 m (2 ft) to 9.0 m (30 ft) form the outside rail as shown in Figure 1. The planer deviation method measures the difference in the slope of the rail crossing between the idealized plane and the actual rail crossing. This method allows for rapid identification of potentially hazardous crossings due to approach slopes that are exceedingly steep.

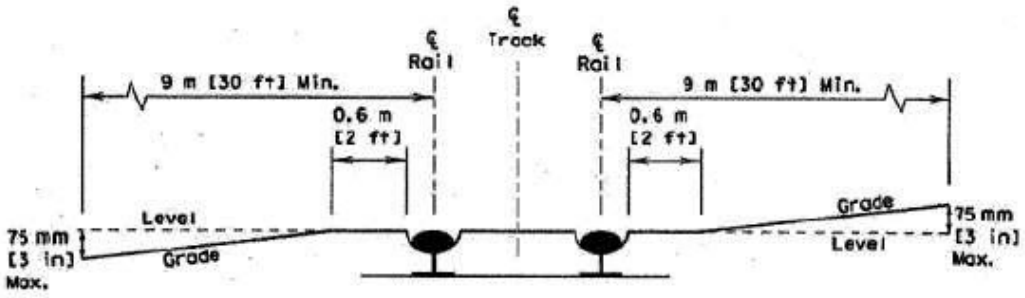

Figure 1: Ideal rail grade crossing geometry from the AASHTO Green Book.

Planer deviation is currently being collected through a rail car based ATIP LiDAR system developed by ENSCO on DOTX 220 and DOTX 304. The Federal Railroad Administration (FRA) has interest in other systems such as Crossing-i which could collect planer deviation data in areas where this data is currently not being collected. This project focused on collecting 30 rail grade crossings by the Crossing-i system and compared to the previously derived planer deviation results collected ENSCO LiDAR system.

Data Collection and Processing

As documented in the Task 2 – Data Collection Technical Briefing the MTRI team collected 31 rail grade crossings in Southeast Michigan (Table 1). Analysis of crossing 000303J – Seltzer Rd was not performed as this crossing was not collected by ENSCO systems. Imagery for each crossing was collected with two

DJI Mavic drones; a Mavic 2 Pro with a 20MP camera and an Enterprise Advanced with a 48MP quad bayer camera. This was done to understand the differences in the data and results to identify the appropriate drone to use for future data collections. These drones were selected due to their ability to be rapidly deployed along with the ability of the M2EA to perform preplanned flight missions which improves efficiency.

Table 1: List of all 31 crossings collected by Crossing ID and crossing street.

Crossing ID	Street	Crossing ID	Street
000114M	State Line Rd.	000220V	William St.
000126G	Samaria Rd.	000239M	Traver Rd.
000129C	Jackman Rd.	000240G	Dhu Varren Rd.
000148G	Gloff Rd.	000243C	Warren Rd.
000149N	Dunbar Rd.	000245R	Northfield Church
000151P	Dixon Rd.	000250M	6 Mile Rd.
000152W	Roosevelt Rd.	000286V	West St.
000165X	Dundee Azalia Rd.	000287C	Alger St.
000170U	Crowe Rd.	000288J	Riddle St.
000177S	Arkona St.	000295U	Allen Rd.
000181G	Willow Rd.	000296B	Oak Grove Rd.
000182N	Platt Rd.	000297H	Sanford Rd.
000184C	Begole Rd.	000303J	Seltzer Rd.
000190F	Warner Rd.	000308T	Richards Rd.
000218U	W. Jefferson Ave.	000310U	Lovejoy Rd.
000219B	Ashley St.		

Processing of the imagery was completed using 3D photogrammetry software on a distributed network. This resulted in reduced processing times compared to a single workstation as the processing for each dataset was distributed between four workstations. This resulted in each Mavic 2 Pro dataset requiring an average of 2.5 hours to complete and M2EA data required 4 hours of computer processing time to complete. The M2EA datasets required more time to process due to more imagery being processed compared to Mavic 2 Pro as a larger area was being collected.

Two sets of point clouds were delivered, the first set was at the full point cloud density and the second was down sampled. The point cloud density for the initial delivery of the Mavic 2 was on average 35,477 points per square meter (ppm^2) and the M2EA was 9,600 ppm^2. With the delivered .laz files being on average 1.5 GB in size, a reduced size point cloud files were requested.

This was achieved through changing the point cloud density of the Mavic 2 to 102 ppm^2 and the M2EA was reduced to 105 ppm^2. The point clouds were also clipped down closer to the extent of the crossings and generally at least 30 ft out from the outside rail along the road and about 50 ft along the rails either side of the crossing. Additional information in the point clouds were also removed to reduce size. This included removing point colors from the saved point clouds. These modifications significantly reduced the size of the .laz files to an average of 1.5 MB.

Comparison of Methods

Planer deviation values were determined from ATIP LiDAR system, manual measured by the ENSCO team, and through a planer deviation tool created by the MTRI team as shown is Table 2. The MTRI planer deviation tool was developed from the Automated Profile Assessment Tool which was developed under the two SBIR phases. This tool works first by automatically identifying the location of the rails, road, and geometry of the crossing from a digital elevation model (DEM) input source. Assessment of the crossing is then performed which identifies areas on the roadway where a vehicle could become hung-up on the crossing based on preset wheelbase and vehicle height parameters. For this research, this tool was adapted to calculate planer deviation instead of vehicle hangup location.

Table 2: Planer deviation values for all 30 crossings using all three methods.

Crossing_ID	Street	ATIP LiDAR (m)	M2EA Manual (m)	Mavic2 Manual (m)	MTRI Tool (m)
000114M	State Line Rd.	0.588	0.540	0.900	0.366
000126G	Samaria Rd.	0.210	0.270	0.280	0.161
000129C	Jackman Rd.	0.200	0.220	0.210	0.433
000148G	Gloff Rd.	0.163	0.160	0.120	0.282
000149N	Dunbar Rd.	0.164	0.350	0.250	0.201
000151P	Dixon Rd.	0.085	0.080	0.230	0.271
000152W	Roosevelt Rd.	0.450	0.530	1.130	0.303
000165X	Dundee Azalia Rd.	0.360	0.410	0.360	2.289
000170U	Crowe Rd.	0.061	0.060	0.030	0.259
000177S	Arkona St.	0.247	0.130	0.180	0.430
000181G	Willow Rd.	0.113	0.200		
000182N	Platt Rd.	0.020	0.050		
000184C	Begole Rd.	0.387	0.370	0.370	0.284
000190F	Warner Rd.	0.299	0.140	0.390	0.233
000218U	W. Jefferson Ave.	0.113	0.110	0.330	0.387
000219B	Ashley St.	0.036	0.090	0.220	0.387
000220V	William St.	0.359	0.430	0.840	0.745
000239M	Traver Rd.	0.330	0.550	0.930	0.393
000240G	Dhu Varren Rd.	0.145	0.150	0.170	0.244
000243C	Warren Rd.	0.164	0.120	0.130	0.129
000245R	Northfield Church	0.790	0.810	0.820	0.316
000250M	6 Mile Rd.	0.088	0.040	0.040	0.054
000286V	West St.	0.172	0.190	0.270	0.124
000287C	Alger St.	0.259	0.340	0.340	0.486
000288J	Riddle St.	0.096	0.210	0.210	0.238
000295U	Allen Rd.	0.330	0.330	0.330	0.132
000296B	Oak Grove Rd.	0.174	0.040	0.080	0.310
000297H	Sanford Rd.	0.226	0.400	0.520	0.248
000308T	Richards Rd.	0.350	0.310	0.340	0.144
000310U	Lovejoy Rd.	0.511	0.780	0.950	0.543

When comparing the manually derived planer deviation values from the drones to the ATIP LiDAR system, the M2EA produced values closer to the ATIP LiDAR system. The average difference in planer deviation value between the M2EA and the ATIP LiDAR is 0.072 m (0.236 ft) and 0.154 m (0.505) for the Mavic 2. These differences in the planer deviation values between the M2EA and the Mavic 2 Pro drones are mostly likely due to the differences in how the imagery was collected and processed. The Mavic 2 Pro was flown at a lower altitude and had a flight path that covered a smaller area more focused on the crossing than the M2EA. This reduced the number of ground control targets available for referencing when processing the Mavic 2 imagery. This allowed for larger errors in geometry and scaling of the point cloud. In some crossings (000152W, 000220V, 000239M, and 000114M) there was up to a 0.36 m (1.18 ft) to 0.60 m (1.97 ft) difference in planer deviation values between the M2EA and Mavic 2. Overall, the M2EA produced results more similar to the ATIP LiDAR at 15 of the crossings while the Mavic 2 produced more similar results at 8 crossings, and they produced the same results at 5 crossings. Two crossings were not collected by the Mavic 2 drone and were only collected with the M2EA due to inclement weather which prevented the data collection.

For the M2EA, 22 of the crossings had less than a 0.10 m (0.328 ft) difference with the ATIP LiDAR with a maximum difference of 0.269 m (0.883 ft) for the 000310U - Lovejoy Rd. crossing. This is a crossing of an unpaved road where only 2.74 m (9 ft) either side of the outside rail are paved in asphalt. The remaining 3.35 m (11 ft) (within the analysis area) of the road is unpaved which is a very dynamic surface compared to concrete or asphalt. Figure 2 shows hillshade representations of point cloud data derived from the M2EA (left) and the ATIP LiDAR (right). These datasets were collected 2 years apart and the unpaved road surface has been graded at least once over that time period. It can easily be seen that there are deep ruts on the southern side of Lovejoy Rd. during the ATIP LiDAR data collection which would have an impact on the planer deviation value. When compared to the road surface from the M2EA data collection, the road surface has been graded to remove the rutting and other distress. This difference alone could account for the 0.269 m (0.883 ft) difference in planer deviation values.

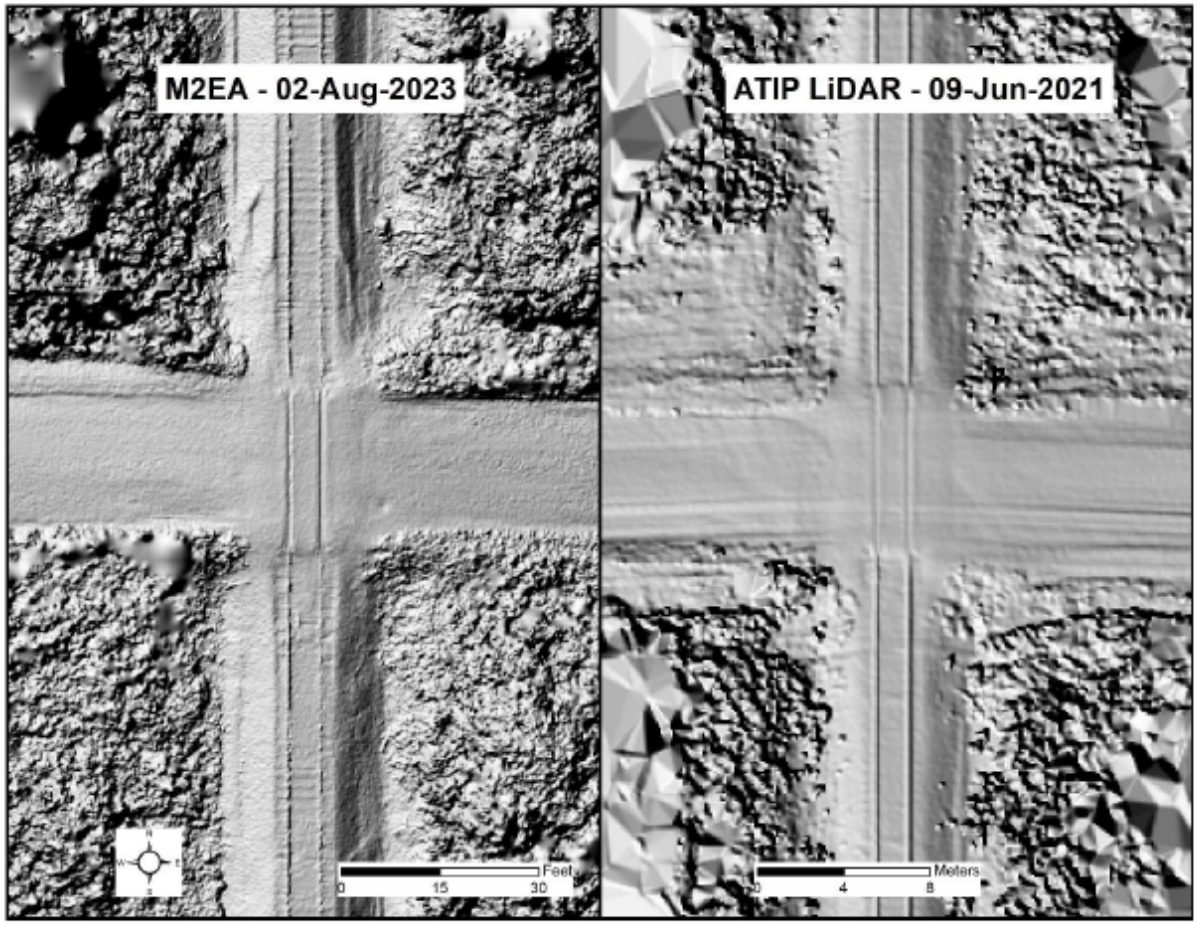

Figure 2: Hillshade representations of the point cloud data from the M2EA (left) and the ATIP LiDAR (right) for the 000310U - Lovejoy Rd. crossing.

The next largest difference in planer deviation values between the M2EA and the ATIP LiDAR is for 000239M - Traver Rd. There is a 0.22 m (0.72 ft) difference in planer deviation values between the two systems and this crossing is an unpaved road as well. Rather than unpaved road distresses (rutting, potholes, or washboarding) it appears that there is some error in the ATIP LiDAR data shown in Figure 3. There are lines of lower elevation radiating from the rail crossing that are not likely to be rutting or other types of distress. This type of elevation difference would cause a difference in planer deviation values similar to normal changes in unpaved road condition between the data collections. The next two crossings with the biggest difference in planer deviation are unpaved roads and they have a difference of 0.186 m (0.61 ft) for 000149N - Dunbar Rd and 0.174 m (0.571 ft) for 000297H - Sanford Rd.

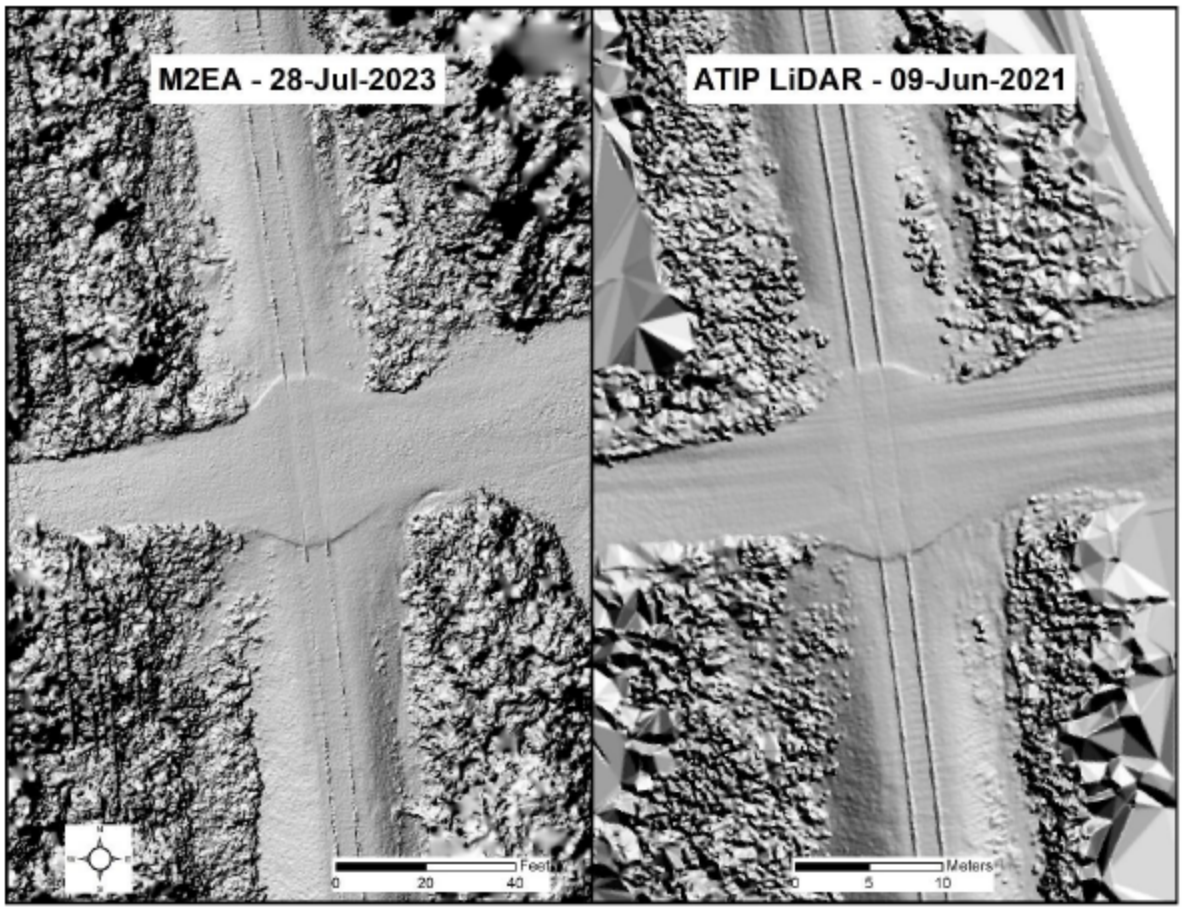

Figure 3: Hillshade representations of the point cloud data from the M2EA (left) and the ATIP LiDAR (right) for the 000239M - Traver Rd. crossing.

The MTRI planer deviation tool was run on the Mavic 2 crossing DEMs. Table 3 shows the difference between the difference planer deviation values from the manually derived Mavic 2 and the MTRI tool. The average difference in planer deviation value is 0.274 m (0.899 ft) with most of the MTRI tools results having at least a 0.10 m (0.328 ft) difference than the manually measured results. This appears to be a function of how the bounding box for the analysis is generated in the MTRI tool. After the crossing has been identified and the crossing geometry has been determined in the tool, a bounding box is generated over the analysis area of the road. In its current version the bounding box may not be generated correctly.

Table 3: Comparison of the planer deviation values of the Mavic 2 data derived from both the manual measurements and the MTRI tool.

Crossing_ID	Street	Mavic2 (m)	MTRI Tool Pro	Manual-MTRI Tool (m)
000114M	State Line Rd.	0.900	0.366	0.534
000126G	Samaria Rd.	0.280	0.161	0.119
000129C	Jackman Rd.	0.210	0.433	0.223
000148G	Gloff Rd.	0.120	0.282	0.162
000149N	Dunbar Rd.	0.250	0.201	0.049
000151P	Dixon Rd.	0.230	0.271	0.041
000152W	Roosevelt Rd.	1.130	0.303	0.827
000165X	Dundee Azalia Rd.	0.360	2.289	1.929
000170U	Crowe Rd.	0.030	0.259	0.229
000177S	Arkona St.	0.180	0.430	0.250
000184C	Begole Rd.	0.370	0.284	0.086
000190F	Warner Rd.	0.390	0.233	0.157
000218U	W. Jefferson Ave.	0.330	0.387	0.057
000219B	Ashley St.	0.220	0.387	0.167
000220V	William St.	0.840	0.745	0.095
000239M	Traver Rd.	0.930	0.393	0.537
000240G	Dhu Varren Rd.	0.170	0.244	0.074
000243C	Warren Rd.	0.130	0.129	0.001
000245R	Northfield Church	0.820	0.316	0.504
000250M	6 Mile Rd.	0.040	0.054	0.014
000286V	West St.	0.270	0.124	0.146
000287C	Alger St.	0.340	0.486	0.146
000288J	Riddle St.	0.210	0.238	0.028
000295U	Allen Rd.	0.330	0.132	0.198
000296B	Oak Grove Rd.	0.080	0.310	0.230
000297H	Sanford Rd.	0.520	0.248	0.272
000308T	Richards Rd.	0.340	0.144	0.196
000310U	Lovejoy Rd.	0.950	0.543	0.407

The largest difference (1.929 m / 6.329 ft) is at 000165X - Dundee Azalia Rd. appears to be the result of an incorrect bounding box. Figure 4 shows that the crossing is not a perpendicular intersection and the road turns right before the crossing. The current version of the tool creates a box extending (30 ft) from the outside rail and does not adjust for a curved road within that distance. For this crossing the bounding box would be extending out beyond the road surface which would cause that large discrepancy.

Figure 4: 000165X - Dundee Azalia Rd. which has a unique crossing geometry with the road curving right before crossing.

Abbreviations and Acronyms

ACRONYM	DEFINITION
AASHTO	American Association of State Highway and Transportation Officials
AREMA	American Railway Engineering and Maintenance-of-Way Association
ATIP	Automated Track Inspection Program
DOTX	Department of Transportation
FHWA	Federal Highway Administration
FRA	Federal Railroad Administration
GPS	Global Positioning System
HPGC	High-Profile Grade Crossing
IMU	Inertial Measurement Unit
LAS	LiDAR Aerial Survey
LAZ	LAS Zip File
LIDAR	Light Detection and Ranging
MTRI	Michigan Technological Research Institute
PMF	Progressive Morphological Filter
SVM	Support Vector Machines